Experimental and Numerical Investigation on Steel Fibrous Reinforced Concrete Slab Strips with Traditional Longitudinal Steel Bars

Arash Pir

Submitted to the
Institute of Graduate Studies and Research
in partial fulfillment of the requirements for the Degree of

Master of Science
in
Civil Engineering

Eastern Mediterranean University
January 2013
Gazimağusa, North Cyprus

Approval of the Institute of Graduate Studies and Research

Prof. Dr. Elvan Yılmaz
Director

I certify that this thesis satisfies the requirements as a thesis for the degree of Master of Science in Civil Engineering.

Asst. Prof. Dr. Murude Çelikağ
Chair, Department of Civil Engineering

We certify that we have read this thesis and that in our opinion it is fully adequate in scope and quality as a thesis for the degree of Master of Science in Civil Engineering.

Asst. Prof. Dr. Serhan Şensoy
Supervisor

Examining Committee

1. Prof. Dr. Özgür Eren _____
2. Asst. Prof. Dr. Giray Ozay _____
3. Asst. Prof. Dr. Serhan Şensoy _____

ABSTRACT

The aim of this thesis was to investigate the influence of steel fibers on mechanical performance of reinforced concrete slab strips based on experimental and theoretical research. Two different types of fibers that are having aspect ratio 60 and 80 have been employed with 4-four diverse volumetric percentages of 0.5, 1.0, 1.5, and 2.0% fibers. All the fibrous specimens have been compared to reinforced concrete slab strips without fibers and with identical longitudinal reinforcement. The flexural tests have been performed on slab strips to examine the effects of fibers on flexural improvement of specimens, and energy absorption enhancement. The dimensions of slab strips have been chosen to observe the flexural failure and prevent the shear failures. The results of experimental study have indicated that presence of fiber has been a significant influence on flexural performance and energy absorption.

In theoretical modeling, by using the constitutive model of material that suggested by previous researchers and standards, the slab strips have been modeled via a FEA software namely, Abacus and analyzed. The results of numerical modeling have illustrated that the constitutive models are compatible with experimental test results quite satisfactorily. The experimental load-deflection curves verified that numerical stress-strain relationships for fibrous concrete material could be utilized for specimen with interaction by traditional reinforcement.

Keywords: Steel fibers, Reinforced concrete, Flexural strength, Energy absorption capacity.

ÖZ

Bu tezin amacı çelik lif kullanılan betonarme plağın mekanik performansının deneysel ve teorik olarak değerlendirilmesidir. Bu amaç doğrultusnda iki farlı narinlik oranına sahip çelik lifler hacimsel olarak yüzde 0.5, 1.0, 1.5 ve 2.0 oranlarında kullanılarak betonarme plaklar deneye tabii tututmuştur edilmiştir. Çelik lifli betonarme plaklar klasik betonarme plak davranışı ile karşılaştırılarak çelik lif oranlarına bağlı mekanik özellikler değerlendirilmiştir. Bu doğrultuda, eğilme momenti etkisinin çelik lif kullanılarak iyileştirilmesi ve göçme durumunda enerji tüketme kabiliyetlerindeki artış irdelenmiştir. Deneyler için hazırlanan betonarme plak boyutu ve kullanılan donatı oranı deney numunelerinde sadece eğilmeye bağlı göçme durumu gözlenecek şekilde şekillendirilip kesme göçmesi önlenmiştir. Deney sonuçları çelik lif kullanımının betonarme plaklarda eğilme kapasitesinde önemli artış sağladığı ve enerji tüketme kapasitesinde de çiddi boyutta bir iyileşme gözlemlendiği görülmüştür.

Teorik çalışma amacı için ise deneyler için hazırlanan numuneler ayni boyut ve yükleme şartlarında ve malzeme davranışı için önerilen bağıntılar kullanılarak Abakus yazılımı vasıtası ile sonlu elemanlar yöntemi ile modellenmiştir. Yapılan analiz neticesinde literatürde önerilen malzeme davranış ilişkilerinin oldukca iyi sonuçlar vermiştir. Deneysel çalışma sonuçları lifli betonlar için önerilen gerilme-birim şekil değiştirme bağıntılarının ayni zamanda klasik betonarme (donatılı) elemanların davranış kapasitesini belirlemede de kullanılabileceği yönunde olmuştur.

Anahtar Kelimeler: Çelik lif, Betonarme, Eğilme Dayanımı, Enerji tüketme kapasitesi.

To Bahman And Mozhgan, My Beloved Parents

ACKNOWLEDGMENT

I owe the greatest appreciation to my supervisor Assistant Professor Dr. Serhan Şensoy. This research has been conducted by Dr. Şensoy guidance and essential advises. Also, I had a brilliant opportunity to get help from Professor Dr. Özgür Eren and I acknowledge his advises for concrete mix-design.

Furthermore, I feel so blessed to have Assistant Professor Dr. Nilgun Hancioglu Eldridge who guided my through thesis writing. A special thanks to Mr. Ogun Kılıç for his assistance in laboratory.

Finally, I share this moment of happiness with my family for their love, moral support and vote of confidence during this research.

TABLE OF CONTENTS

ABSTRACT iii

ÖZ iv

DEDICATION vi

ACKNOWLEDGMENT vii

LIST OF TABLES xi

LIST OF FIGURES xii

LIST OF ABBREVIATIONS xv

LIST OF SYMBOLS xvi

1 INTRODUCTION 1

1.1 Background 1

1.2 Objective 2

1.3 Scope 3

1.4 Significance 4

2 BACKGROUND INFORMATION AND LITERATURE REVIEW 5

2.1 Introduction 5

2.2 Previous studies 5

2.2.1 SFRC constitutive concept in compression 5

2.2.2 SFRC tension models 9

2.2.3 SFRC without conventional reinforcement 11

2.2.4 SFRC and traditional reinforcement 14

3 METHODOLOGY 17

3.1 Introduction 17

3.2 Experimental module 17

3.2.1 Specimens provision 17

3.2.2 Flexural Test Setup 21

3.2.3 Compressive Test Setup 24

3.3 Numerical study and modeling module 25

3.3.1 Finite Element Modeling 25

3.3.2 Energy Absorption 30

4 RESULT ANALYSIS AND DISCUSSION 31

4.1 Experimental results of flexural test until 10 mm deflection. 31

4.1.1 Reinforced Slab Strips without fiber 33

4.1.2 Fibrous Reinforced Slab Strips with Aspect Ratio 80 (AR80) 33

4.1.3 Fibrous Reinforced Slab Strips with Aspect Ratio 60 (AR60) 37

4.1.4 Flexural Energy Absorption 42

4.2 Experimental results of flexural test until Concrete Collapse 43

4.2.1 The flexural test until reaching the maximum deflection 43

4.3 Numerical Simulation of Slab Strips 48

4.3.1 Effect of meshing size on numerical result 48

4.3.2 Numerical and experimental load-deflection results 51

4.4 Compressive Test Results 57

4.5 Results discussion summary 58

5 CONCLUSION AND PERSPECTIVES 59

5.1 Conclusions 59

5.2 Future Studies 61

REFERENCES 62

LIST OF TABLES

Table 1. Concrete and SFRC mix proportions 18

Table 2. Steel Fibers Characteristics 18

Table 3. Average Energy Absorption 42

Table 4. Ultimate Energy Absorption 47

LIST OF FIGURES

Figure 1. Zaragoza Bridge Pavilion (Rieder) 2

Figure 2. Industrial Jointless Floor (Twintec) 2

Figure 3. Simplified SFRC Tensile Model by (Sujivorakul, 2012) 10

Figure 4. Idealized compressive model for SFRC 12

Figure 5. Idealized tensile model of SFRC 12

Figure 6. Idealized Fibrous concrete constitutive model according to RILEM (2003) 13

Figure 7. Schematic reinforced beams shape (1bar) 20

Figure 8. Slab strip moulds and specimens 20

Figure 9. Schematic drawing of flexural test apparatus 21

Figure 10. Flexural Test Apparatus 22

Figure 11. Displacement gauges 23

Figure 12. Inelastic strain definition in Abaqus 27

Figure 13. Tensile Stress-Cracking strain relationship in Abaqus 28

Figure 14.3D Model of Slab Strip in Abaqus 30

Figure 15. General Load-Displacement Diagram-Zone A: Elastic Deformation, Zone B: Crack Propagation, Zone C: Entirely cracked condition 32

Figure 16. Load- Deflection Diagram: RC Slab without Fibers 33

Figure 17. Load- Deflection Diagram: RC Slab 0.5% Fiber (AR80) 34

Figure 18. Load- Deflection Diagram:RC Slab 1.0% Fiber (AR80) 35

Figure 19. Load- Deflection Diagram: RC Slab 1.5% Fiber (AR80) 35

Figure 20. Load- Deflection Diagram: RC Slab 2.0% Fiber (AR80) 36

Figure 21. Comparative Load- Deflection Diagrams:With and without fibers (AR80) 37
Figure 22. Flexural Enhancement Trend (AR80) 37
Figure 23. Load- Deflection Diagram:RC Slab 0.5% Fiber (AR60) 38
Figure 24. Load- Deflection Diagram:RC Slab 1.0% Fiber (AR60) 39
Figure 25. Load- Deflection Diagram:RC Slab 1.5% Fiber (AR60) 39
Figure 26. Load- Deflection Diagram:RC Slab 2.0% Fiber (AR60) 40
Figure 27. Comparative Load- Deflection Diagrams:With and without fibers (AR80) 41
Figure 28. Flexural Enhancement Trend (AR60) 42
Figure 29. Average Energy Absorption 43
Figure 30. Typical load-unloading-deflection diagram 44
Figure 31. Typical trend fit line 44
Figure 32. Compressive Collapse of Concrete 45
Figure 33. Comparative Load- Deflection Diagrams (Until Concrete Collapse): With and without fibers (AR80) 45
Figure 34. Comparative Load- Deflection Diagrams (Until Concrete Collapse): With and without fibers (AR60) 46
Figure 35. Load-Time diagram during the analysis with divers meshing sizes of slabs 48
Figure 36. Stress distribution in slab strips: a- 51000 meshes, b- 22600 meshes 49
Figure 37. Steel Reinforcement stress distribution 50
Figure 38. Theoretical and experimental curves- Slab Strips without fiber 51
Figure 39. Theoretical and experimental curves- Slab Strips with 0.5% Fiber (AR80) 52

Figure 40. Theoretical and experimental curves- Slab Strips with1.0% Fiber (AR80) 52
Figure 41. Theoretical and experimental curves- Slab Strips with 1.5% Fiber (AR80) 53
Figure 42. Theoretical and experimental curves- Slab Strips with 2.0% Fiber (AR80) 53
Figure 43. Theoretical and experimental curves - Slab Strips with 0.5% Fiber (AR60) 54
Figure 44. Theoretical and experimental curves - Slab Strips with 1.0% Fiber (AR60) 55
Figure 45. Theoretical and experimental curves - Slab Strips with 1.5% Fiber (AR60) 56
Figure 46. Theoretical and experimental curves - Slab Strips with 2.0% Fiber (AR60) 56
Figure 47. Stress-strain graphs for specimens with AR80 Fiber 57
Figure 48. Stress-strain graphs for specimens with AR60 Fiber 57

LIST OF ABBREVIATIONS

AR60	Aspect Ratio 60
AR80	Aspect Ratio 80
FEA	Finite Element Analysis
FEM	Finite Element Method
FRC	Fibrous Reinforced Concrete
SFRC	Steel Fibrous Reinforced Concrete

LIST OF SYMBOLS

ε_{c0}	Strain at peak concrete compressive strength
ε_c	Concrete compressive strain
E_{c1}	Initial young's modulus of concrete
E_{ci}	Concrete secant modulus of elasticity
f_{cm}	Average compressive strength
l_f	Effective length of fiber
d_f	Fiber diameter
σ_c	Concrete compressive strength
V_f	Volume percentage of fibers
W_f	Weight fraction of fibers

Chapter 1

INTRODUCTION

1.1 Background

Since biblical era, brittleness was a disfavor property of building materials such as clay bricks or other mortars. Primitive men attempt to enhance materials performance by adding the straw or horse hair to them. These were the fundamental fibrous components in the history.

In about 1900, the asbestos was utilized as the reinforcement of cement paste in Hatschek process for producing the pipes or roof plates and subsequently, glass fibers are suggested for reinforcing the pastes by Biryukovichs (Brandt, 2008) . There were considerable amount of researchers who investigated the behavior of FRC in modern history, but Romualdi and his colleagues had the significant impact on steel fibers reinforced concrete researches. In about 1960, two papers were published by Romualdi which orientated the researchers towards SFRC's world (Zollo, 1997).

Contemporary definition of SFRC is referred to a fibrous concrete composite which consists of hydraulic cementitious material, discrete steel fibres, and aggregates. (ACI544, 1999)

Nowadays, SFRC is employed to construct structures which are exposed to corrosive environment, critical natural catastrophes or affected by dynamic loads. Compared to conventional concrete, SFRC has enhanced endurance and mechanical properties. There are some examples of SFRC structures which were constructed around the world:

Figure 1. Zaragoza Bridge Pavilion (Rieder)

Figure 2. Industrial Jointless Floor (Twintec)

1.2 Objective

In this research, influence of type and percentage of fibers on flexural behavior of reinforced thin slabs with low longitudinal bars ratio have been investigated.

Furthermore, effects of fibers on energy consumption of reinforced slab without any shear resist element are examined to assess the enhancement of fibers utilization.

1.3 Scope

This investigation is categorized into two stages which are experimental and numerical works. In the initial part, diverse thin slab strips are casted according to the same mix design but various percentages and type of fibers, and low longitudinal reinforcement ratio. The fiber's percentage ranges from 0.0 to 2.0 percent with aspect ratio of 60 and 80. These samples are subjected to displacement-controlled load and stress-controlled load. Their restraints are pin-support and the deflection record on middle of span.

In the theoretical phase, Abaqus (Simulia Abaqus/CAE 6.11, 2011) software is used to simulate reinforced concrete strips by considering constitutive models which are suggested by previous researchers and calculated values from the experimental part.

Abaqus (Simulia Abaqus/CAE 6.11, 2011) and Mathematica (Wolfram-Research-Inc., 1988-2011) are employed in numerical module of this research. Abaqus is one of most powerful tools in FEA and Extended FEA which bases on constitutive models of materials and dynamic/explicit or standard/implicit solvers for various analytical cases. Mathematica is functional programming software with predefined Equations for evaluate the energy absorption and interpolating the experimental data.

1.4 Significance

According to ACI318 utilization of fibers for enhancement of mechanical properties of concrete as a structural material is restricted to shear strength improvement under several limitations, and the SFRC flexural enhancement, compared with normal concrete is not approved by building codes (ACI544, 2002). However, in thin slabs with minimum allowable flexural reinforcement, the flexural capacity of section could be affected by fibres significantly and this enhancement would not be a minor effect.

Furthermore, high energy absorption is a desirable characteristic of any construction material. This property could be improved by adding the fibers to plain concrete. In this research, amelioration of energy absorption due to diverse percentages and types of fibers is investigated.

To consider the mechanical improvement of fibers, their effects have been examined to assess magnitude of this enhancement.

Chapter 2

BACKGROUND INFORMATION AND LITERATURE REVIEW

2.1 Introduction

Technically, research has been done on SFRC which could be categorized into two basic fields, i.e. mechanical rheology and material serviceability investigations.

The SFRC mechanical rheology has been examined by various researchers for providing the constitutive models of compressive or tensile zone, flexure and shear capacity data, and etc. In this chapter, significant studies on SFRC are reviewed in order to prepare a sufficient background of this research.

2.2 Previous studies

2.2.1 SFRC constitutive concept in compression

Mangat and M. Azarit (1984) examined the effects of steel fibers on concrete in compressive zone. As a result of that research, it was declared that compared to plain concrete, there was an increase of 27% in initial cracking stress by adding 3% of steel fibers. Furthermore, steel fiber significantly decreased the level of critical stress and reduced initiation of critical stress in concrete. The strain capacity, i.e. volumetric and longitudinal, at elementary and critical level of stress reduced significantly due to fibres. Up to stress equal to 60% of the ultimate stress, Poisson's

ratio and lateral strain were not influenced by fibers; however, beyond this stress level, these values were escalated markedly (Mangat & Motamedi Azarit, 1984).

Barros and Figueiras (1999) based on Mebarkia and Vipulanandan (1993) model, purposed the following expression to represent SFRC constitutive model in compression:

$$\sigma_c = f_{cm} \frac{\frac{\varepsilon_c}{\varepsilon_{C0}}}{(1-p-q)+q\left(\frac{\varepsilon_c}{\varepsilon_{C0}}\right)+p\left(\frac{\varepsilon_c}{\varepsilon_{C0}}\right)^{\frac{1-q}{p}}} \tag{2.1}$$

with

$$q = 1-p-\frac{E_{C1}}{E_{ci}} \tag{2.2}$$

$$p+q \in]0,1[\tag{2.3}$$

$$\frac{1-q}{p} \rangle\ 0 \tag{2.4}$$

In these Equations, ε_{C0}, f_{cm}, E_{C1}, and E_{ci} are the strain at peak stress, compressive strength, initial elasticity modulus, and secant modulus, respectively. The recommended value and expressions for ε_{C0} and p which are suggested by Barros & Figueiras (1999) according to different types of fibers are:

$$\left.\begin{aligned}\varepsilon_{c0} &= \varepsilon_{c00} + 0.00026 \cdot W_f \\ p &= 1.0 - 0.722\exp(-0.144 \cdot W_f)\end{aligned}\right\} \text{ for aspect ratio 75} \qquad (2.5)$$

and

$$\left.\begin{aligned}\varepsilon_{c0} &= \varepsilon_{c00} + 0.0002 \cdot W_f \\ p &= 1.0 - 0.919\exp(-0.394 \cdot W_f)\end{aligned}\right\} \text{ for aspect ratio 60} \qquad (2.6)$$

where W_f is the percentage weight of fibers in mixture (Barros & Figueiras, 1999) .

According to CEB-FIP Model Code, strain at peak stress for plain Concrete and secant elasticity modulus are demonstrated as following expressions (Telford, 1993)

$$\varepsilon_{c10} = 2.2 \times 10^{-3} \qquad (2.7)$$

$$E_{ci} = 21500 \times \left(\frac{f_{cm}}{10}\right)^{1/3} \qquad (2.8)$$

$$E_{c1} = \left(\frac{f_{cm}}{\varepsilon_{c1}}\right)^{1/3} \qquad (2.9)$$

Ezeldin and Balaguru (1992) proposed a compressive model of SFRC based on Carreira and Chu (1985). They derived an analytical model of stress-strain for SFRC which corresponded with material parameter β. β is a coefficient that is defined regarding weight fraction and fiber aspect ratio (Equation 2.13). According to this research following Equation was provided for compressive constitutive model.

$$\frac{\sigma_c}{f_c} = \frac{\beta\left(\frac{\varepsilon_c}{\varepsilon_{pf}}\right)}{\beta - 1 + \left(\frac{\varepsilon_c}{\varepsilon_{pf}}\right)^{\beta}} \tag{2.10}$$

$$\beta = \left(1.093 - 0.7132 \cdot w_f \cdot \frac{L_f}{D_f}\right) \tag{2.11}$$

$$\varepsilon_{pf} = \varepsilon_{c0} + 446 \cdot 10^{-6}\left(w_f \cdot \frac{L_f}{D_f}\right) \tag{2.12}$$

Junior et al. (2010) redefined the parameters β according to the volumetric participation of fibers in Equation 2.13 and ε_{C0} respectively to volumetric fraction of steel fibers and compressive strength. (Junior, et al., 2010)

$$\beta = \left(0.0536 - 0.5754 \cdot V_f\right) f_c \tag{2.13}$$

$$\varepsilon_{c,0} = \left(0.00048 + 0.01886 V_f\right) Ln\left(f_c\right) \tag{2.14}$$

Furthermore, Nataraja et al. (1999) purposed a numerical model for stress-strain of SFRC which were based on Carreira and Chu (1985) model. In this research, crimped end fibers were used and following parameters were defined to describe the constitutive model. (Bencardino, Rizzuti, Spadea, & Swamy, 2008)

$$f_{cf} = f_c + 3.51\left(RI\right) \tag{2.15}$$

$$\varepsilon_{pf} = \varepsilon_{c0} + 0.0006\left(RI\right) \tag{2.16}$$

$$\beta = 0.5811 + 1.93(RI)^{-0.7406} \tag{2.17}$$

$$RI = w_f \cdot \frac{L_f}{D_f} \tag{2.18}$$

where W_f defined as weight percentage of fibers, ε_{C0}= 0.002, and L_f/D_f as fibers

Aspect ratio.

Bencardino et al.(2007) collated several SFRC stress-strain models and concluded that failure strain of SFRC was higher than 0.0035 which adopted in current codes. In addition, SFRC samples consist of 1.6% and 3.0% of fibers, exhibit a residual stress of 74 and 78% of their ultimate stress at 0.01 strain (Bencardino, Rizzuti, Spadea, & Swamy, 2008).

2.2.2 SFRC tension models

A modified direct tensile model was propesed by Naaman (2003) which based on Valle and Buyukozturk (1993) by considering concrete cylindrical compressive strength (f'_c) and fiber factor (F). This model provided a simplified post-cracking behavior of SFRC. According to this model residual tensile stress for hooked fiber is calculated by following expression

$$f_r = 0.2 \cdot \sqrt{f'_c} \cdot F \tag{2.19}$$

$$F = V_f \frac{L_f}{D_f} \cdot \beta \tag{2.20}$$

which β in Equation 2.20 is the bond factor and value of 1.0 was reported by Campione et al., V_f is percentage of steel fibers and $\frac{L_f}{D_f}$ is the aspect ratio of fiber which is used in concrete (Meskenas & Ulbinas, 2011).

An idealized direct tensile model for SFRC is purposed by C. Sujivorakul (2012) which based on experimental research on hooked fibers with aspect ratio of 65 and 80 (Figure 3). In this study, the tensile rheology of concrete was divided into pre-cracking and post-cracking zone. Following expressions are defined the tensile model respectively to volumetric fiber content (Sujivorakul, 2012).

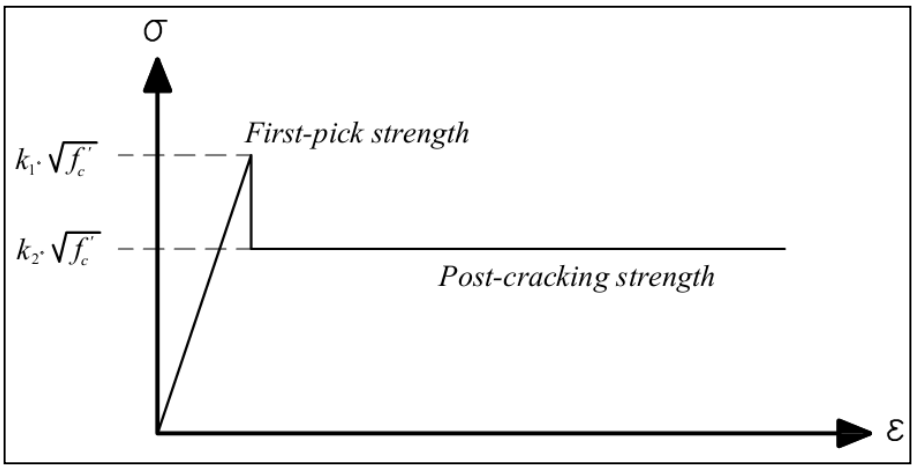

Figure 3. Simplified SFRC Tensile Model by (Sujivorakul, 2012)

$$\sigma_f = k_1 \cdot \sqrt{f'_c} \tag{2.21}$$

$$\sigma_p = k_2 \cdot \sqrt{f'_c} \tag{2.22}$$

$$k_1 = 0.3481 + 0.1329 \cdot V_f \tag{2.23}$$

$$k_2 = \left(-0.001V_f{}^2 + 0.0038V_f\right) \times \frac{L_f}{D} \times \left(L_f\right)^{0.2} \quad (2.24)$$

These formulas are obtained from samples which subjected to direct tension test and lower boundary was recommended by the author.

2.2.3 SFRC without conventional reinforcement

An experimental research on flexural behavior steel fibrous reinforced concrete slabs was carried out by Khaloo and Afshari (2005). Their experimental program included 28 slabs with dimension of 820×820×80 mm. The fibers content ranges from 0.5% to 1.5%. According to this research, the energy absorption of SFRC slab with 0.5%, 1.0%, 1.5% of steel fibers were 12, 24, and 48 times higher respectively, compared to energy absorption of plain concrete slabs. Furthermore, it was recommended to use 0.75 to 1.75 percent of fiber to improve energy absorption of concrete (Khaloo & Afshari, 2005).

The behavior of SFRC members subjected to bending force is investigated by Barros and Figueiras (1999). SFRC strips with mesh and different percentage of fiber are examined and a significant improvement in flexural capacity of slabs was observed. According to experimental result, the ultimate flexural strength of slab with 60 kg/m^3 fiber content was twice a slab with plain concrete (Barros & Figueiras, 1999).

A design method for slabs which are subjected to bending force is suggested by Soranakom and Mobasher (2009). In this suggestion, idealized tensile model and stress-strain relationship have been used (Figure 4, Figure 5).

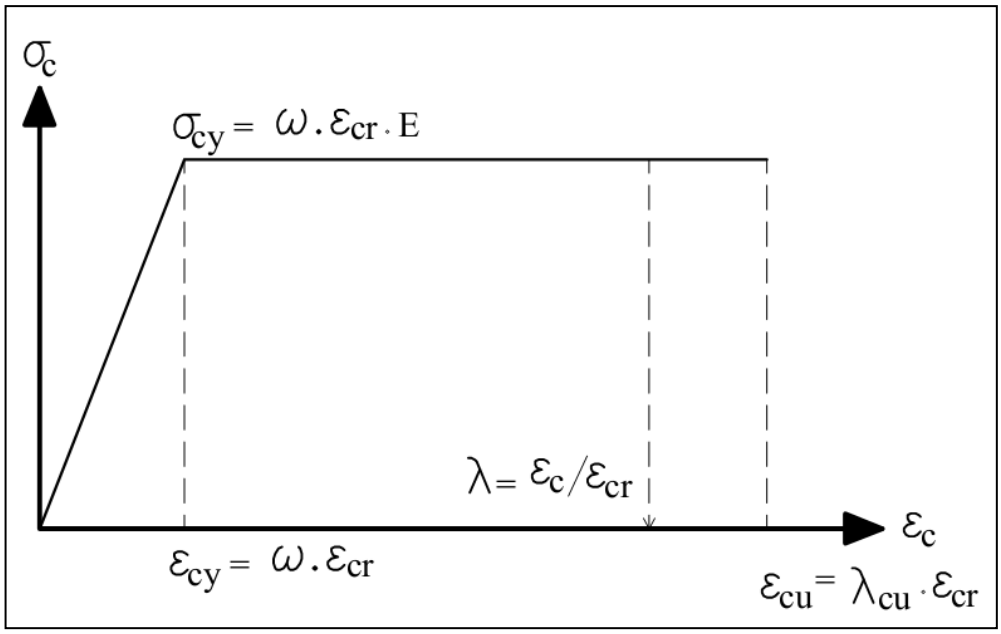

Figure 4. Idealized compressive model for SFRC

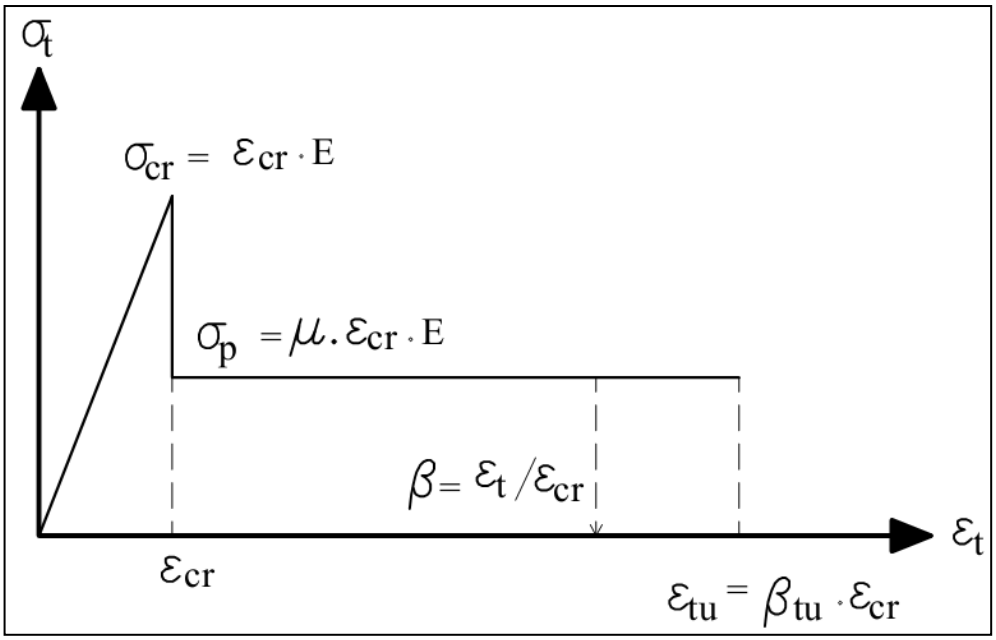

Figure 5. Idealized tensile model of SFRC

In these models, ***E*** is elasticity modulus which is calculated by following formula according to ACI 318-11.

$$E = 4700 \cdot \sqrt{f'_c} \text{ (MPa)} \qquad (2.25)$$

Strain at first cracking, ε_{cr}, is defined as the strain which is maximum elastic deformation in tensile zone. Parameter μ, represents the post-cracking strength proportional to cracking stress, σ_{cr}, which ranges from 0.0 to 1.0. Compressive zone is introduced by an elastic part and perfect plasticity behavior. Parameter, ω, stands for ratio of compressive strain to ε_{cr}. In this research, RILEM (1999) idealized constitutive model has been used to provide essential data for identifying the related parameters (Figure 6).

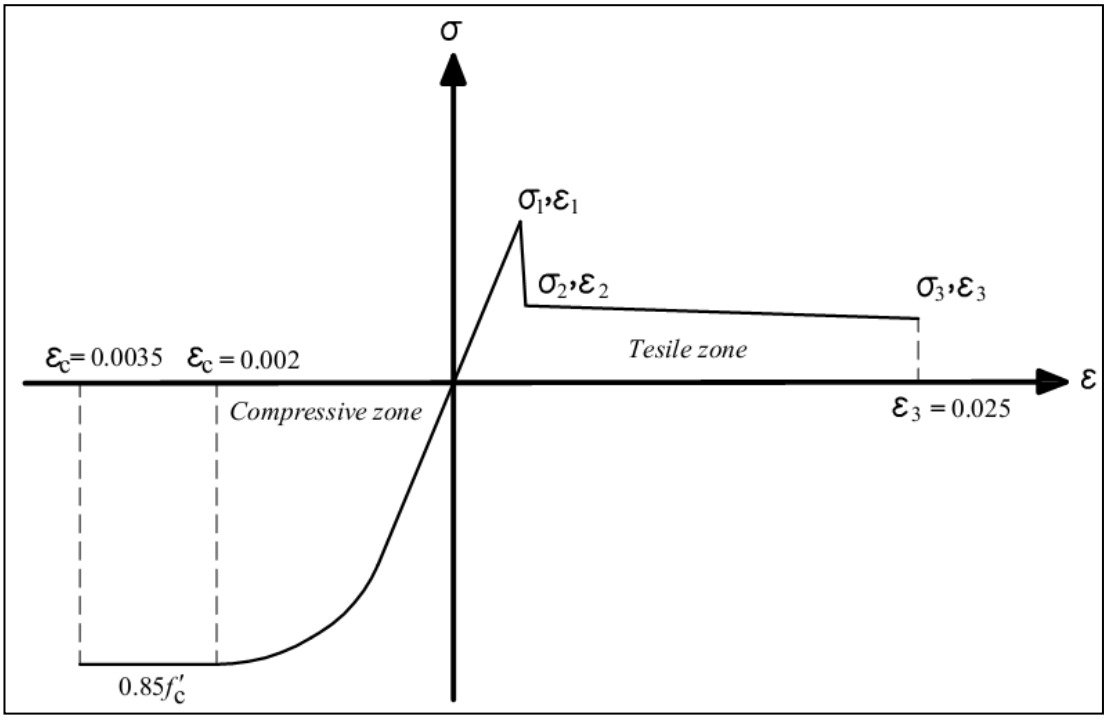

Figure 6. Idealized Fibrous concrete constitutive model according to RILEM (2003)

According to the constitutive SFRC model of RILEM (2003), ultimate strain in tension, ε_3, is assumed 0.025 and in compression, ε_{cu}, is restricted to 0.0035. By considering these assumptions, constitutive parameters to SFRC idealized design model are defined as following expressions (Soranakom & Mobasher, 2009).

$$\sigma_{cr} = E \cdot \varepsilon_{cr} = 0.56 \cdot \sqrt{f'_c} \text{ (SI Units)} \tag{2.26}$$

$$\varepsilon_{cr} = \frac{\sigma_{cr}}{E} = 118 \cdot 10^{-6} \tag{2.27}$$

$$\sigma_{cy} = 0.85 \cdot f'_c \text{ (MPa)} \tag{2.28}$$

$$\mu = \frac{\sigma_p}{E \cdot \varepsilon_{cr}} \tag{2.29}$$

$$\omega = \frac{\varepsilon_{cy}}{\varepsilon_{cr}} = 1.52 \cdot \sqrt{f'_c} \text{ (SI Units)} \tag{2.30}$$

$$\beta_{tu} = \frac{\varepsilon_{tu}}{\varepsilon_{cr}} \approx 212 \tag{2.31}$$

$$\lambda_{tu} = \frac{\varepsilon_{cu}}{\varepsilon_{cr}} \approx 30 \tag{2.32}$$

2.2.4 SFRC and traditional reinforcement

The mechanical behavior of combined SFRC and conventional longitudinal bars was examined by several researchers. The structural member which subjected to examination was tunnel linings slab. The purposed model of bending-cracking width represented the significant increase in cracking width. According to this research, presence of steel fibers provides variety of advantage in durability and ultimate state limits. In addition, the minimum reinforcement was influenced by presence of fibers (Chiaia, Fantilli, & Vallini, 2009).

In 1999, there has been an experimental research on combination of SFRC and conventional rebar, with 3 various steel bars ratio and two different percentages of steel fibers. Flexure capacity enhancement was reported as 7.52% and 26.43% respective to 0.5 and 1.0 per cent of fiber content. According to this research, additional flexural capacity does not depend on rebar ratio and compressive strength influence on flexural enhancement is more significant (Ashour, Wafa, & Kamal, 2000).

A combined experimental investigation and numerical analysis of SFRC and traditional reinforcement was conducted by group of researchers in 2009. In the numerical research, ANSYS (Ver. 2003) was used by researchers, and according to their report, relevant stress-deflection and crack propagation were observed. Besides, boundary conditions and zero deformation points were verified the numerical modeling (Özcan, Bayraktar, Sahin, Haktanir, & Türker, 2009).

As a flexural experiment result, a considerable increase in bending toughness and flexural capacity at ultimate state were reported for SFRC reinforced beams which were in concrete class of C20-30 and fibers' dosage of 30 and 60 kg/m^3. In lower concrete class (C20), the better enhancement rate of bending toughness was observed. In addition, the improvement in ultimate flexural capacity in class C30 was reported (Altun, Haktanir, & Ari, 2007).

An inverse method was proposed as an alternative model for stress-strain of SFRC by using the moment-curvature of reinforced concrete beams. According to Gribniak et al. (2012), the application of this tensile model in smeared cracking model is widely acceptable. For this purpose, equivalent tensile model has to be utilized and

residual stresses are calculated respective to cracking width. (Gribniak, Kaklauskas, Hung Kwan, Bacinskas, & Ulbinas, 2012)

The bond between concrete and rebar has been affected by presence of fibers. According to R.P. Dhakal and Song (2005) research on various percentage of fiber influence on bonding leads to less significant concrete-rebar interaction in SFRC beams (Dhakal & Song, 2005).

In 2010, a theoretical investigation on effects of fiber types on anchorage of steel fibers has been conducted. According to this research, the failure in fibrous section would be a result of deforming the hooked-end fibers, and the empirical coefficients for anchorage of fibers have been suggested. (Šalna & Marčiukaitis, 2010)

Chapter 3

METHODOLOGY

3.1 Introduction

This investigation has concentrated on two modules, i.e. experimental examination and analytical modeling of thin slab strips. In the experimental module, due to facilities and dimension restrictions, semi real-scale specimens have been casted to evaluate the influence of steel fiber proportion on mechanical response of RC beams.

In the numerical module, all types of reinforced SFRC beams has been modeled to measure experimental results against the theoretical models which were suggested by other researchers (Barros & Figueiras, 1999), (Sujivorakul, 2012). Abaqus (Simulia Abaqus/CAE 6.11, 2011) was employed as FEA tool, due to its compatibility with inelastic behavior of concrete. To determine the numerical data of concrete for simulation, and also for energy absorption calculation, also the symbolic language namely, Mathematica (Wolfram-Research-Inc., 1988-2011) was used in this study.

3.2 Experimental module

3.2.1 Specimens provision

3.2.1.1 Concrete and SFRC mix design

The desirable strength of concrete in this research was 30 MPa for standard cylindrical specimen. According to ACI318-11, ultimate strength of cylindrical specimen is equal to 85 per cent of cube specimen (ACI318, 2011); therefore, by considering the number of trials and specimens, the design compressive strength was

assumed 35 MPa. Cement class was 32.5 and crushed limestone coarse aggregate with maximum size of 10 mm was chosen. It was decided to design self-compacting paste. For this purpose, the slump was assumed 150 mm and 0.5 per cent super plasticizer has been used. By using the admixture, slump of plain concrete mixture was about 270 mm. The concrete has been designed according to Building Research Establishment (BRE) guideline (Marsh, 1988). Steel fiber's volumetric percentages were 0.5, 1.0, 1.5, and 2.0 by volume of concrete. Summarized proportions are listed in below (Table 1).

Table 1. Concrete and SFRC mix proportions

No.	Water (kg)	Cement (kg)	W/C	FA (kg)	CA (kg)	Adm. (kg)	Fiber (kg)	Fiber (Vol%)
1	220	400	0.55	1062	718	4	0.00	0.0
2	220	400	0.55	1062	718	4	39.25	0.5
3	220	400	0.55	1062	718	4	78.50	1.0
4	220	400	0.55	1062	718	4	117.80	1.5
5	220	400	0.55	1062	718	4	157.00	2.0

Two types of hooked-end steel fibers have been employed in this research, which were Dramix ZP305 and RC-80/50-BN. Aspect ratio is defined as effective length over diameters of fiber. The characteristics of fibers are demonstrated in Table 2 .

Table 2. Steel Fibers Characteristics

Fibers Types	Effective length (mm)	Diameter (mm)	Tensile Strength (MPa)	Density (kg/m^3)	Aspect Ratio (l/d)
60/30	30	0.500	1345	7850	60
80/50	50	0.625	1270	7850	80

The mixing of proportions was commenced by adding coarse aggregate, fine aggregate, and the cement. Dry content was blended for 1 minute. Subsequently, water and super plasticizer have been added to mixture simultaneously. After that, fibers have been added gradually to avoid balling and segregation. Total time for mixing the fresh concrete was approximately 8 minutes to separate the fibers completely.

3.2.1.2 Specimen preparation, casting, and curing

There were 12 cubic trials for compressive strength of mix-designs that had been casted and tested regarding the maximum fibers content and type of fibers. The target strength had been observed with a slight diversity.

Although, according to the hand calculation, the dimensions of concrete strips and the experiment setup were suitable for this study, before casting the main specimens, four reinforced concrete strips with and without fibers were casted to ensure that the failure of the specimens were in pure flexural zone, and the samples had not been collapse due to shear failure. The flexural failures in all trials had been observed.

There were two different specimens, i.e. reinforced slab strips and cubes. The dimensions of beam were 100 mm by 1100 mm by 200 mm and 150 mm cube molds were used (Figure 7, Figure 8). Longitudinal steel ratios have been used according to the minimum value for concrete slabs (1ϕ8). The cover for reinforcement was 20 mm according to ACI318-11.

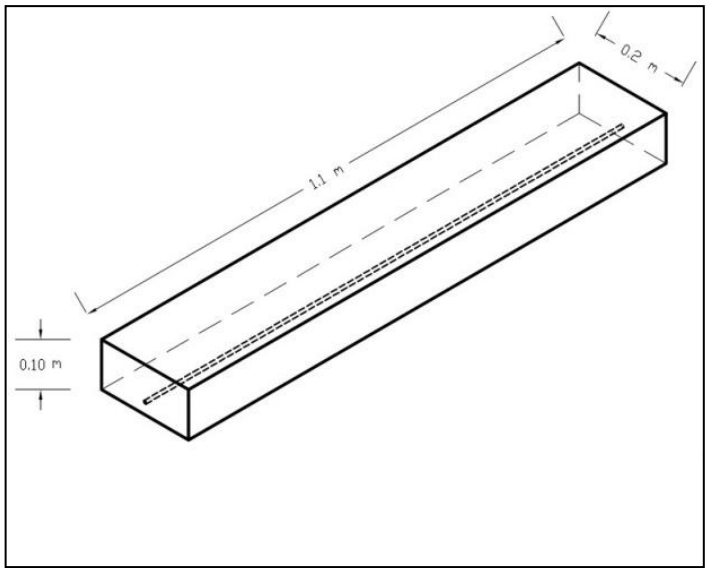

Figure 7. Schematic reinforced beams shape (1bar)

As it is mentioned in previous section, super plasticizer has been employed to increase the workability of mixture. Although, the 0.5 percentage of cement content was assumed as the amount of superplasticizer, the plain concrete mix and SFRC mixes with low amount of fibers reflected the self compacting behavior of concrete and extra vibration was not necessary; for the 1.5 and 2.0 volumetric per cent of fibers, there has not been sufficient workability and it was unavoidable to utilize the vibrating table and poker.


Figure 8. Slab strip moulds and specimens

After casting the beams and cubes samples, the specimens has been kept for 24 hours in the laboratory moisture and subsequently, placed in water curing tanks. Total duration of curing for specimens was 28 days.

3.2.2 Flexural Test Setup

3.2.2.1 Test Apparatus

To investigate the flexure behavior of SFRC, a pure flexural zone is required. For this purpose, the slab strips were subjected to two symmetrical loads which provided a region without any shear force and torque. To increase the amount of moment at middle span of strip and reduce the shear stresses, the span between supports and loading point was 400 mm and pure flexure region had the length of 200 mm. the schematic drawing of apparatus is illustrated in Figure 9 and Figure 10.

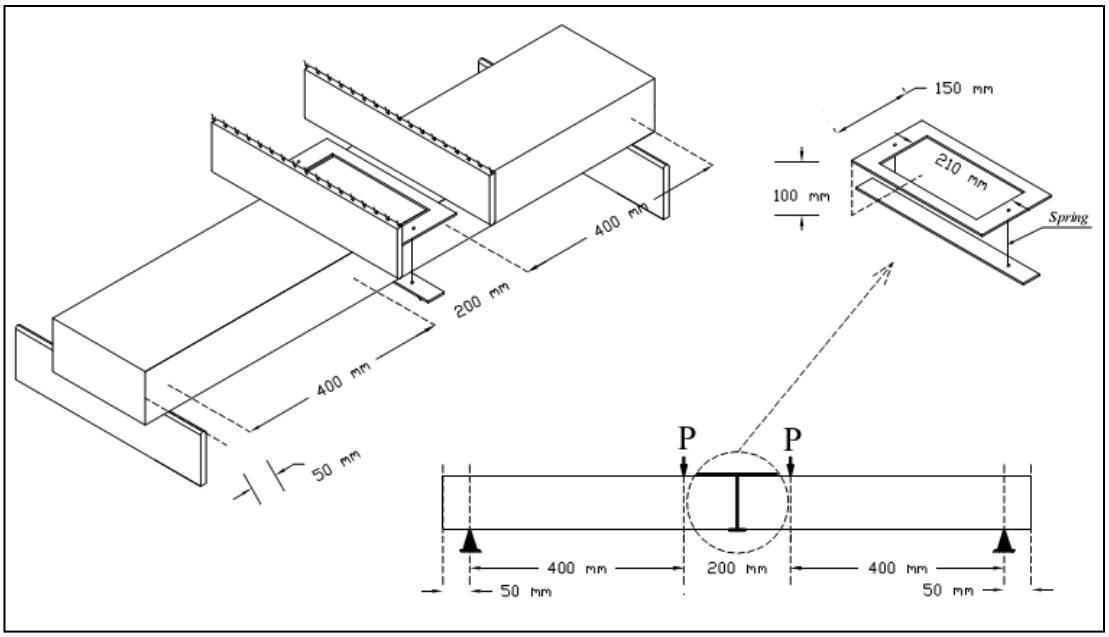

Figure 9. Schematic drawing of flexural test apparatus

In Figure 11, a steel frame which is connected to a steel band by a spring has been shown. The application of this part is to transfer the middle deflection to the sensors.

The reason for using the springs instead of steel rods was to minimize the side effects of steel frame on flexural strength of slabs beams.

The loading procedure has been displacement-controlled with 1 mm/min rate. The load rate has been chosen by considering the trial test results. The trial beams had been examined with 0.5, 1.0, and 2.0 mm/ min speed rate, and subsequently, the 1.0 mm/min were utilized in this investigation.

Figure 10. Flexural Test Apparatus

3.2.2.2 Data Collectors

There was a critical restriction on examination of concrete strips with ToniTechnik (Model 2071) machine. The displacement sensors of this machine were limited to record 10 mm displacement. Although, in all cases before 10 mm mid-span deformation the longitudinal reinforcement had been yielded, the compressive crashing of concrete did not occur, and the yielding of steel bar could not be accepted as the collapse of reinforced concrete strips. Therefore, recording the load-

displacement data after 10 mm deformation was a primary requirement for accurate investigation.

The first idea to reach to concrete fracture and recording the data was to shift form displacement-control loading to stress-control loading after 10 mm settlement of concrete strip mid-span. Subsequent to changing the loading method, a camera could be used to record the deformation. The primary issue regarding this method was variety of loading rate, the machine could apply the load by stress-control and it was not possible to synchronize the load and displacement directly and the load had to be recorded manually. This method provides the acceptable results but it had less accuracy than the complete displacement-control loading. Therefore, the parallelization of two data logger has been designed for this experiment.

Figure 11. Displacement gauges

The final decisions for performing the flexural experiment of slab strips were displacement-control loading and unloading procedure with the fixed loading rate,

utilization of an extra data logger, and data synchronization. In this method, ToniTechnik (Model 2071) and data logger had to be parallelized, and vital point in parallelization was identical data recording rate of these machines. Hence, the time interval of both instrument set as 1.0 second (minimum time interval of data logger). The capacity of deformation gauge of data logger instrument was 50 mm.

Before each test, the gauges of both machines placed on the steel band (There were 4 gauges, each side of strip 2 gauges - Figure 11), and all the initial displacement values were made zero. Instantaneously, the data logger was executed and it was working continuously. After that the ToniTechnik (Model 2071) machine had been executed. The data were recorded by both data loggers until the ToniTechnik (Model 2071) gauges capacity (10 mm) and then ToniTechnik (Model 2071) only has been stopped and specimen has been unloaded, the ToniTechnik (Model 2071) gauges had been modified and again they started to record new load-displacement data. During the experiment the data logger did not stop tracing of slab strip deformations. The Figure 11 illustrates the schematic data that were provided by these two data logger.

3.2.3 Compressive Test Setup

For each mix-design 6 cubes have been casted. The cube dimensions are 150 mm. Each series of cubes have been examined for 7 and 28 days after casting according to ASTM C0039. Although in ASTM code, the cylindrical specimen was suggested for examination, according the several researches it is possible to use cubes as test specimens, and the result of compressive strength test of concrete cylinder is about 80 to 90 per cent of concrete cube (Shetty, 2005).

The load-rate ranges from 0.15 to 0.35 MPa/s according to ASTM C0039. (ASTM-C39, 2004)

3.3 Numerical study and modeling module

In the numerical simulation of slab strips, the Abaqus (Simulia Abaqus/CAE 6.11, 2011) and Mathematica (Wolfram-Research-Inc., 1988-2011) had been utilized. Mathematica was employed to produce the input data for Abaqus, and also to evaluate the energy absorption of each specimen.

3.3.1 Finite Element Modeling

3.3.1.1 Concrete in Abaqus Package

For defining the concrete mechanical properties in Abaqus (Simulia Abaqus/CAE 6.11, 2011), two theorems are considered to simulate the non-linearity of concrete, i.e. the Inelastic behavior of concrete in compression and secondly, the tensile behavior of brittle material which are related to cracking of them. To define the mechanical behavior of plain and fibrous concrete, the concrete stress-strain formula which is purposed by Barros (1999), was used due to its compatibility with fiber types of this research. (Barros & Figueiras, 1999)

This formula that is introduced in Chapter 2 (Equation 2.1) represents the influence of fibers on the strength of concrete and its relevant strain. Input data for this constitutive model is weight percentage of fibers and average strength of cylindrical concrete specimen in compression. In this case, the cube compressive strength and volume percentage of fibers converted to cylindrical compressive strength and weight percentage of fibers in concrete content.

To describe the concrete material, the initial modulus of elasticity was defined according to Equation (2.10). Subsequently, ‘Concrete Damaged Plasticity’ (CDP) which is based on inelastic rheology of concrete under compression and tension was

defined. To identify the CDP parameters, the plasticity, compressive, and tensile behavior of concrete data were perquisites. The plasticity of concrete data was defined according to report by Eriksson & Gasch (2010) and Abaqus recommendation.

In the next step, compressive modulus, yielding stresses and their relevant strains according to Barros model by using Mathematica (Wolfram-Research-Inc., 1988-2011) prepared and defined. In Figure 12, the relationship between inelastic strain and yielding stress is shown.

Subsequently, the tensile models of plain and fibrous concrete were defined according to cracking strains and their relevant tensile stresses. Majority of the tensile models are divided into pre-cracking and post-cracking condition of concrete. According to the literature review, the tensile models which were conducted by direct tensile test provide the idealized post cracking stress. In this research, the post cracking behavior of concrete is simulated according to RILEM model (2003), simplified tensile model by C. Sujivorakul (2012), and the minimum tensile stress in SFRC that was purposed by Naaman (2003). In RILEM model the maximum tensile strain of fibrous concrete is limited to 0.025, and the tensile cracking strain in elastic zone is 0.0012. The tensile stresses for elastic and cracked section that are suggested by C. Sujivorakul (Equation 2.21 and 2.22) were applied in this investigation as a most recent tensile model. The minimum post-cracking stress in the tensile constitutive model represent in Chapter 2 (Equation 2.19) based on Naaman (2003) research.

In the finite element modeling, the tensile model defined as stress-cracking strain model. Figure 13 illustrates the schematic tensile model in this research.

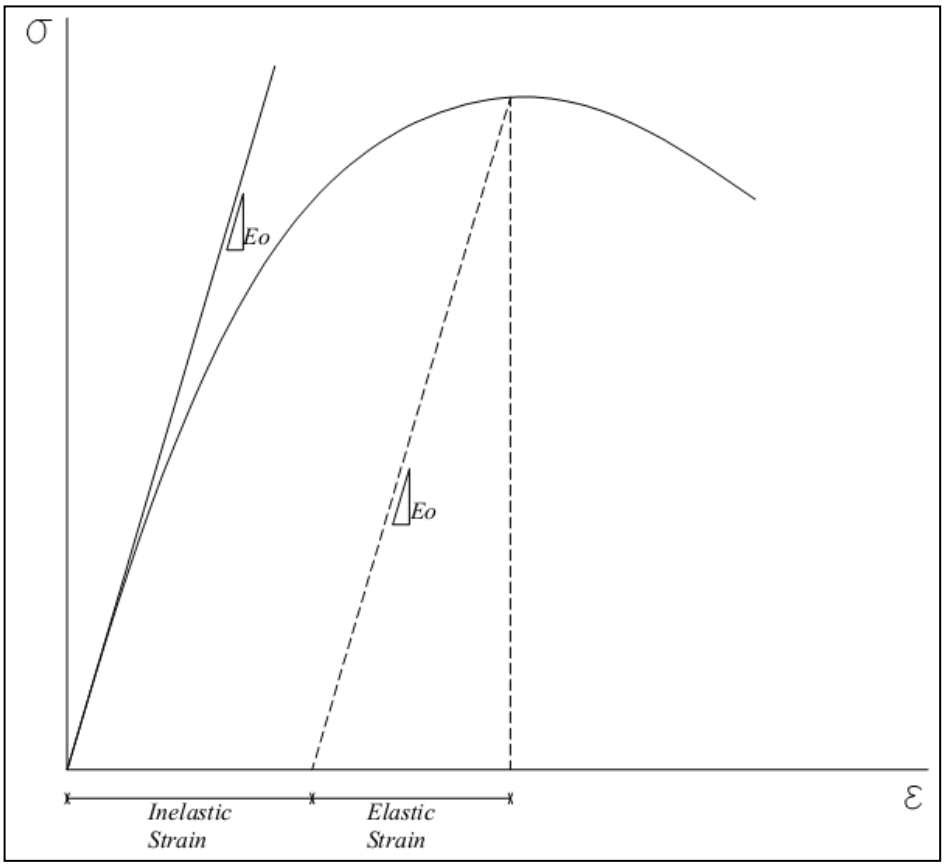

Figure 12. Inelastic strain definition in Abaqus

3.3.1.2 Steel in Abaqus

Compared to concrete, steel mechanical properties are not complicated due to its isotropic and elastic behavior. According to experimental result, the yielding stress of steel was 440 MPa and ultimate strength of steel was 580 MPa. The modulus of elasticity of steel bar is defined as ideal steel which is equal to 210 GPa. Generally, the steel characteristic represents by an idealized model according to Prabir recommendation (Basu, Shylamoni, & Roshan, 2004).

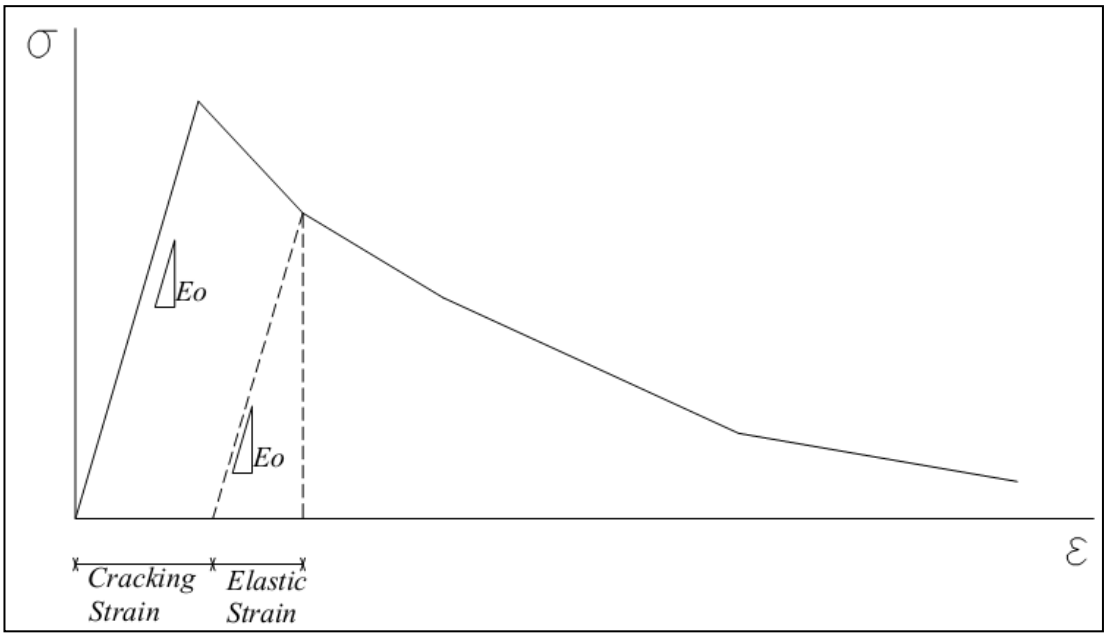

Figure 13. Tensile Stress-Cracking strain relationship in Abaqus

3.3.1.3 Concrete and Steel Bars Element Types in Abaqus

The hexahedral and quadrilateral elements have been applied as concrete strips and longitudinal reinforcement elements respectively. The concrete elements were 3D solid, and reinforcement has the membrane characteristic to wave all flexural effect of steel bars on the section. In the Abaqus (Simulia Abaqus/CAE 6.11, 2011), there is another way to model reinforcement which is based on wire modeling, since the wire modeling does not provide information regarding the stresses and strains in steel, membrane member has been used to model the reinforcement.

3.3.1.4 Interaction between concrete and longitudinal reinforcement in Abaqus

Modeling the interaction between different materials could affect the whole analysis, and defining the contact between concrete and steel has various should be done carefully. The friction stresses between materials, normal contact between surfaces, and several parameters are required as contact properties. In addition, there has been an order in Abaqus to define the interaction between steel rebar and concrete with default properties. In this method, in the interaction module, reinforcement defined

as an embedded region in concrete beam, and by using this property the influence of mesh size has been minimized by automatic contact defining. (Hibbit, Karlsson, & Sorensen, 2009)

3.3.1.5 Loading procedure, convergence, and analysis method

According to Abaqus (Simulia Abaqus/CAE 6.11, 2011) manual user, to apply the displacement-control load, there have been three way to define the load. The first method is defining a displacement that its amplitude has been change during the analysis, but it could lead to a warning in status file due to risk of incompatibility in boundary condition in initial step. The second type of displacement-control loading is to define the load as velocity. The final way for applying the load is to define acceleration during the analysis at the specified points; however, this method definitely affects the result because of inertia forces. In this research, displacement-load has been defined as velocity due the complete compatibility with explicit analysis.

In Abaqus, there are diverse analysis techniques such as Risk/Statics, Static/Implicit, Dynamic/Explicit, and etc. In this investigation the Dynamic/Explicit analysis has been employed to simulate the experimental procedure.

Explicit analysis is efficient numerical analysis of large models with relatively small dynamic response intervals and for the discontinuous analysis procedures. Explicit type of analysis provides very general contact and boundary conditions and utilizes a consistent, large-deformation theory (Simulia Abaqus/CAE 6.11, 2011).

Convergence in finite element method is the primary issue during the analysis. The initial step to avoid convergence problems is to use different mesh sizes for steel bar

and concrete beam that prevent the stress concentration due to coincidence of elements nodes (Eriksson & Gasch, 2010).

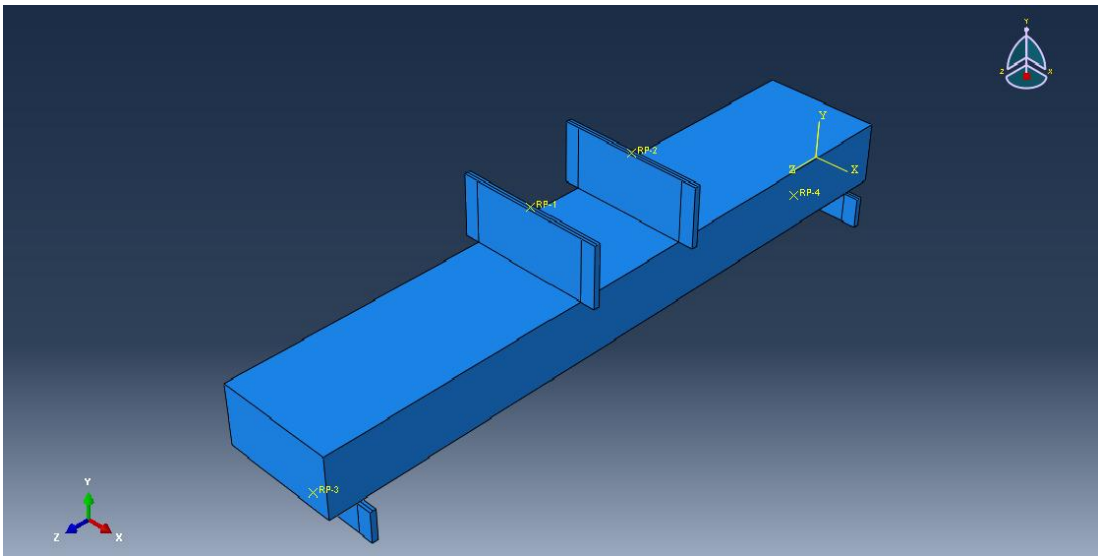

Figure 14.3D Model of Slab Strip in Abaqus

In Figure 14, the 3D model of slab strips has been shown. There are two rigid plates for applying the displacement-loads that resemble to the experiment setup and also 2 rigid plates defined as supports.

3.3.2 Energy Absorption

The quantity of energy absorption is measured by area under load-deflection diagram, and it is an important index in seismic characteristic of concrete members. However the energy absorption is defined as ability of absorbing the energy under impact load, the integration of load-deformation curve under a monotonic load represents the similar mechanical behavior.

In current research, the integration of curves from experimental results have been calculated by numerical method via Mathematica (Wolfram-Research-Inc., 1988-2011).

Chapter 4

RESULT ANALYSIS AND DISCUSSION

In this section, several comparative results of experimental load-deflection curves have been provided and discussed. These discussions focus on the effect of fiber dosage and type on flexural behavior of slab strips with low longitudinal bar ratio Post-cracking rheology of fibrous reinforced slab strips has been presented in respect to fiber aspect ratio and dosages. Furthermore, toughness (flexural energy absorption) of slab strips that illustrates the influence of fibers on the concrete slabs has been investigated.

4.1 Experimental results of flexural test until 10 mm deflection.

All specimens were subjected to 10 mm displacement load in middle of strips, and 9 diverse load-deformation diagrams have been introduced as the results of flexural test, which are reinforced slab strip and fibrous reinforced slab strips with aspect ratio 80 and 60. Each diagram has three vital zones that represent elastic (un-cracked), crack propagation, and entirely cracked condition (Figure 15).

The elastic zone in each diagram would be affected by load rate critically, and higher load rate leads to higher initial elastic deformation (Figure 15-Zone A). By increasing the load after the elastic zone, the tensile stresses in concrete exceed the cracking stress and the flexural stiffness of slab decrease suddenly subsequent to crack propagation. As it demonstrates in previous chapter, the slab strips were subjected to a displacement- controlled load. In zone B, the magnitude of load has

been declined suddenly to control the displacement rate by apparatus due to abrupt decrease in the slab stiffness. With each stage of crack development, a drop in load has been observed.

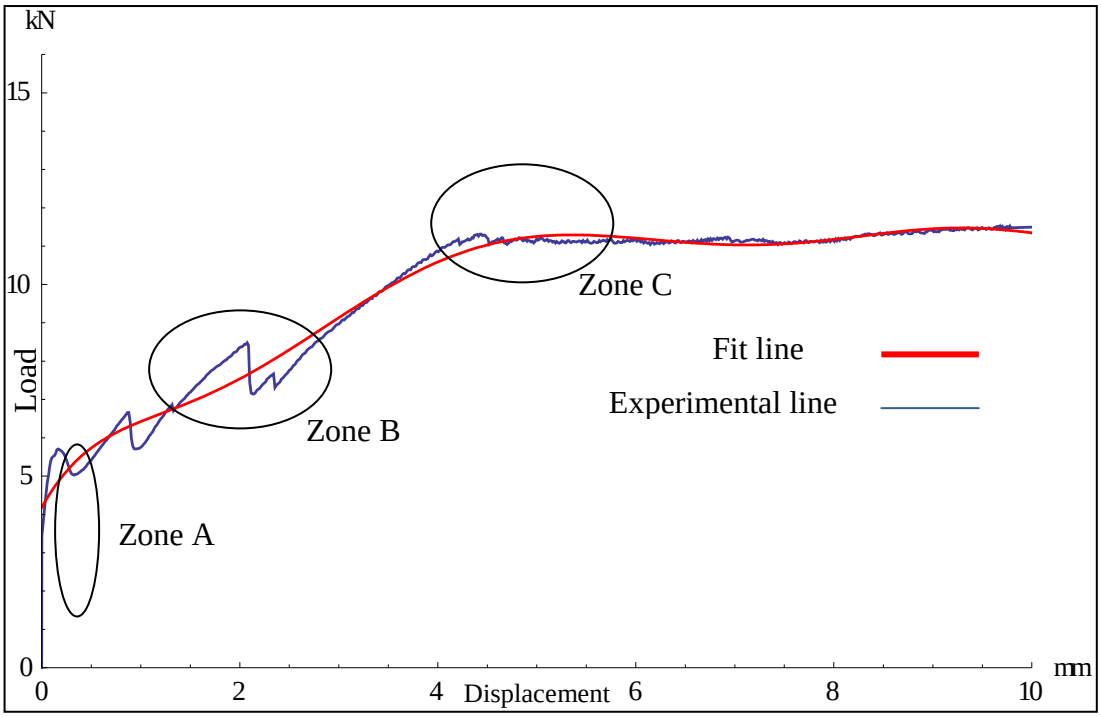

Figure 15. General Load-Displacement Diagram-Zone A: Elastic Deformation, Zone B: Crack Propagation, Zone C: Entirely cracked condition

Totally cracked condition stands for ultimate flexural strength and initiation of post-cracking performance (Zone C). In this zone, the longitudinal reinforcement is yielded and the compressive strain in concrete is increased until collapsing the concrete in compression. Generally, in investigation of flexural behavior of slabs and beams in ultimate strength condition the tensile stresses in concrete were neglected because the cracked section could not transfer tensile forces, but presence of steel fibers maintains the tensile properties, and concrete are able to convey tensile forces through the fibers.

To establish a comparative result discussion and to avoid vague diagrams, average fit lines have been used in the graphs. The reasons for using these fit lines are to prevent from disordered and unorganized curves, and to provide comprehensible figures; especially, in collation of load-displacement curves for diverse percentages of fibers.

4.1.1 Reinforced Slab Strips without fiber

Three specimens has been examined as the traditional slab strips, during the spreading cracks, several keen drops have been detected. An average fit line between the values has been derived from experimental results.

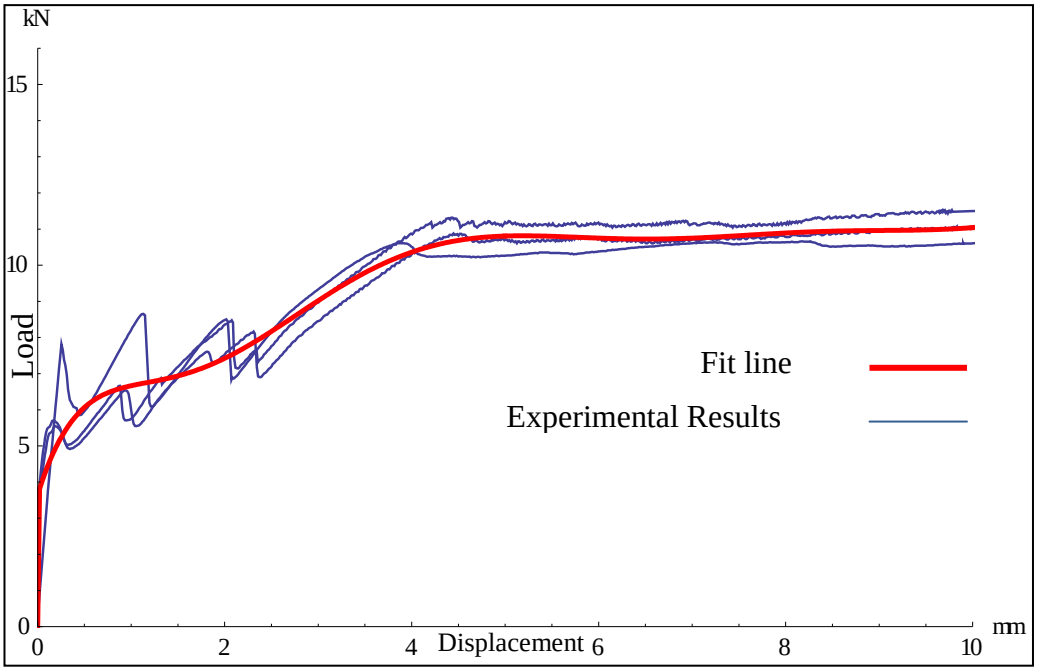

Figure 16. Load- Deflection Diagram: RC Slab without Fibers

4.1.2 Fibrous Reinforced Slab Strips with Aspect Ratio 80 (AR80)

The primary effect of fibers on load-deflection of RC Members appears at crack propagation stage (Figure 15-zone B). Utilization of 0.5 percentage fiber does not affect the abrupt stiffness loss. By increasing in fiber percentage, the scale of drops

in diagrams would be reduced, and by using 1.5 and 2.0 % fiber, there won't be any significant sudden reduction in stiffness (Figure 19 and Figure 20).

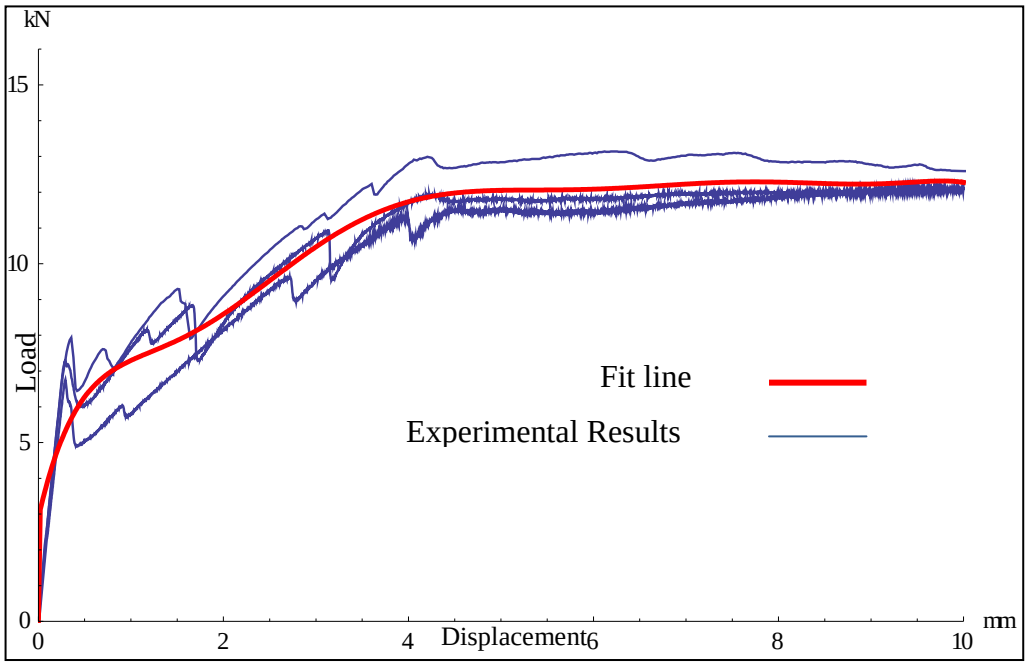

Figure 17. Load- Deflection Diagram: RC Slab 0.5% Fiber (AR80)

The effect of fiber on flexural strength of slab strips have been examined, and according to experiment outcomes, 1.5 and 2.0 % fibers content in concrete have the maximum flexural enhancement. However the improvement rate in 2.0% fibers has been reduced.

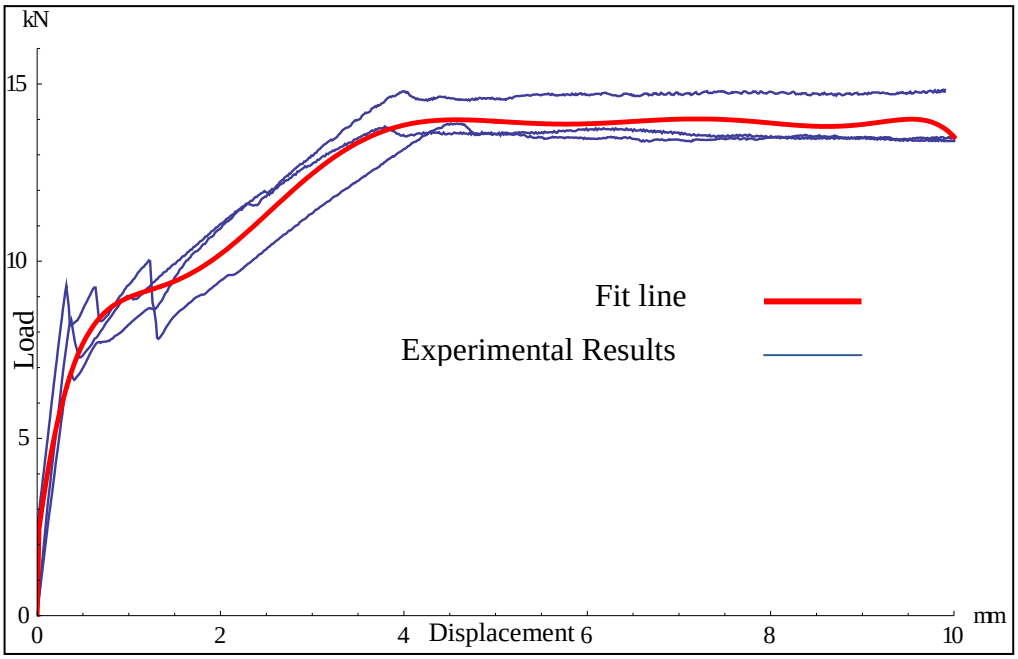

Figure 18. Load- Deflection Diagram:RC Slab 1.0% Fiber (AR80)

Specimens with 0.5, 1.0 per cent fiber and without fibers have not shown any decrease in flexural strength, in the contrary, slab strips with 1.5 and 2.0 percentages of fibers have a slight decrease in flexural performance after pick point.

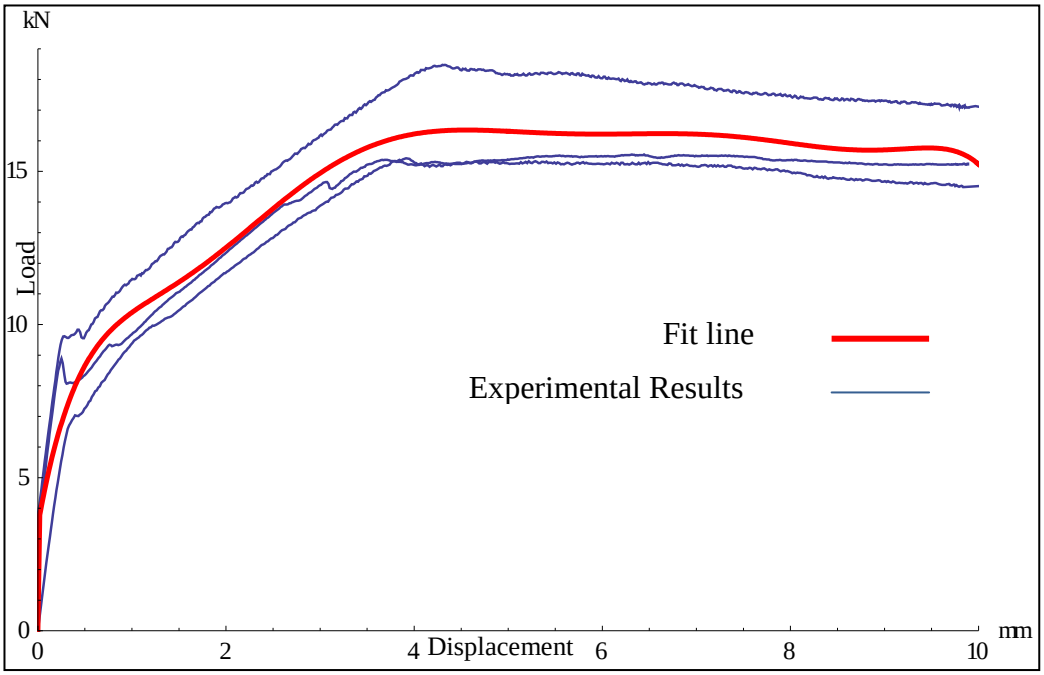

Figure 19. Load- Deflection Diagram: RC Slab 1.5% Fiber (AR80)

The comparative load-displacement curves for diverse percentage of fibers have been shown in Figure 21. The average fit lines have been employed in this Figure to clarify the difference between specimens and according to experimental results, the flexural strength variation between 1.5 and 2.0 per cent steel fiber was not considerable. In addition, the flexural stiffness of each specimen somehow related to the slope of its fit line, and higher stiffness during the crack propagation is a result of higher fiber dosage in concrete mixture. However, this mechanical aspect in 1.5 and 2.0% of fibers is identical.

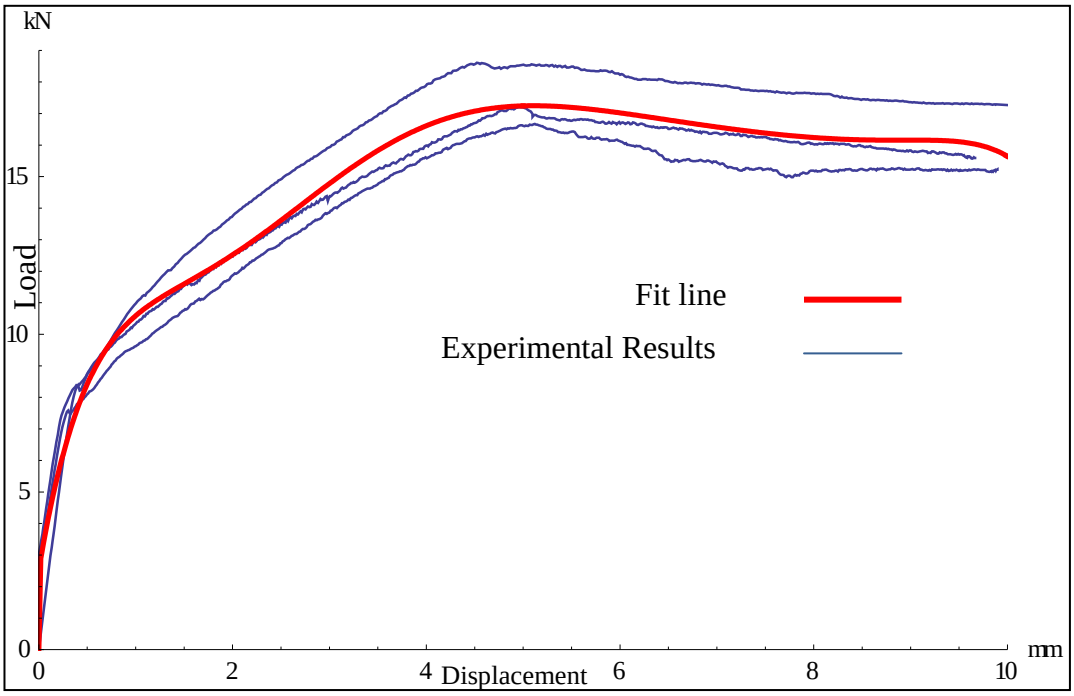

Figure 20. Load- Deflection Diagram: RC Slab 2.0% Fiber (AR80)

The flexural strength enhancements in regard to fiber percentage were illustrated in Figure 22.

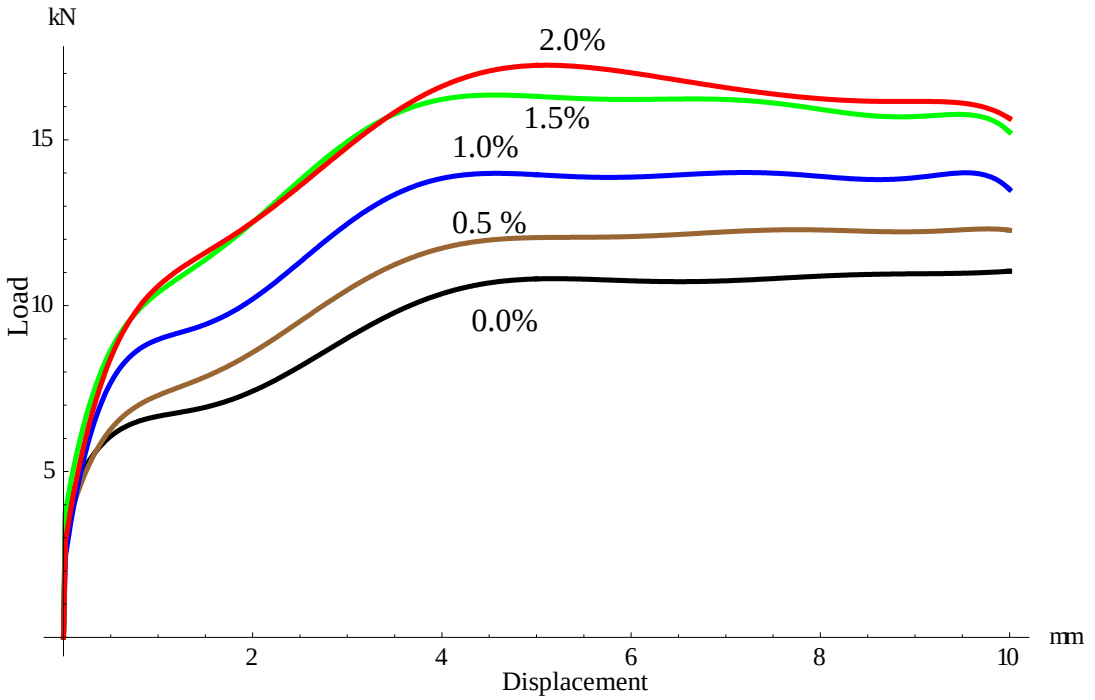

Figure 21. Comparative Load- Deflection Diagrams:With and without fibers (AR80)

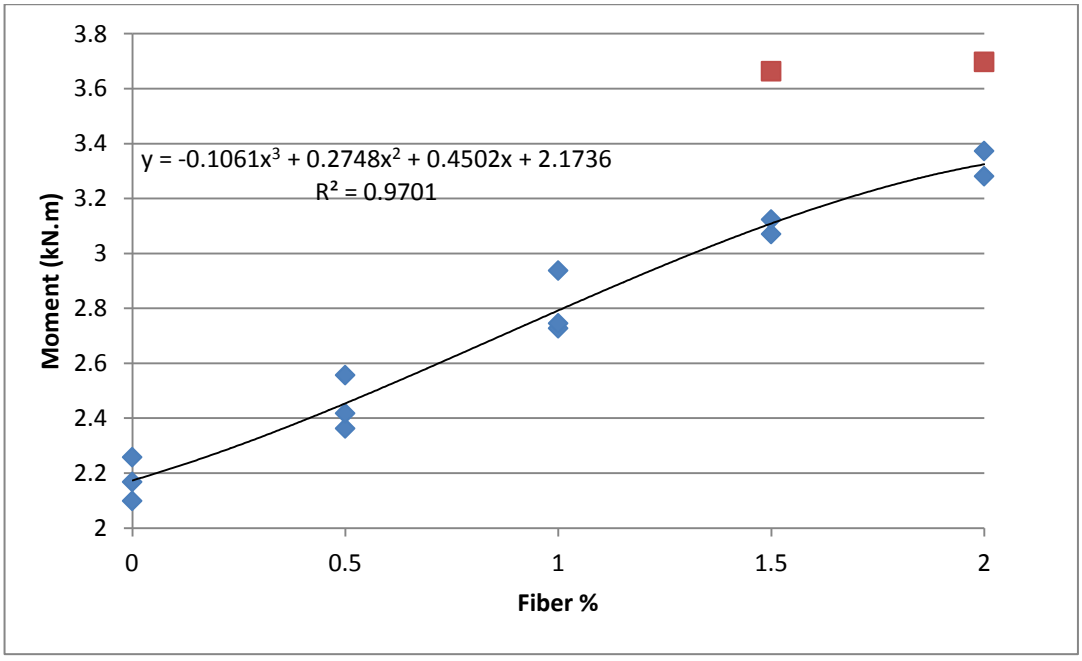

Figure 22. Flexural Enhancement Trend (AR80)

4.1.3 Fibrous Reinforced Slab Strips with Aspect Ratio 60 (AR60)

Utilization of fibers with aspect ratio 60 has the similar influence on crack propagation as fiber with aspect ratio 80. Half per cent fiber in slab strip has not

decreased the crack spreading significantly (Figure 23), but slabs with higher percentage of fiber, have exhibited less drops in stiffness.

In this research, for each fibrous reinforced slab strips with aspect ratio 60 fibers, only two specimens have been casted and examined. Although, it could be more logical to employ 3 samples, however due to close results of two examinations, the interpolation between data leads to acceptable mean value to evaluate the fiber effects on reinforced concrete slabs.

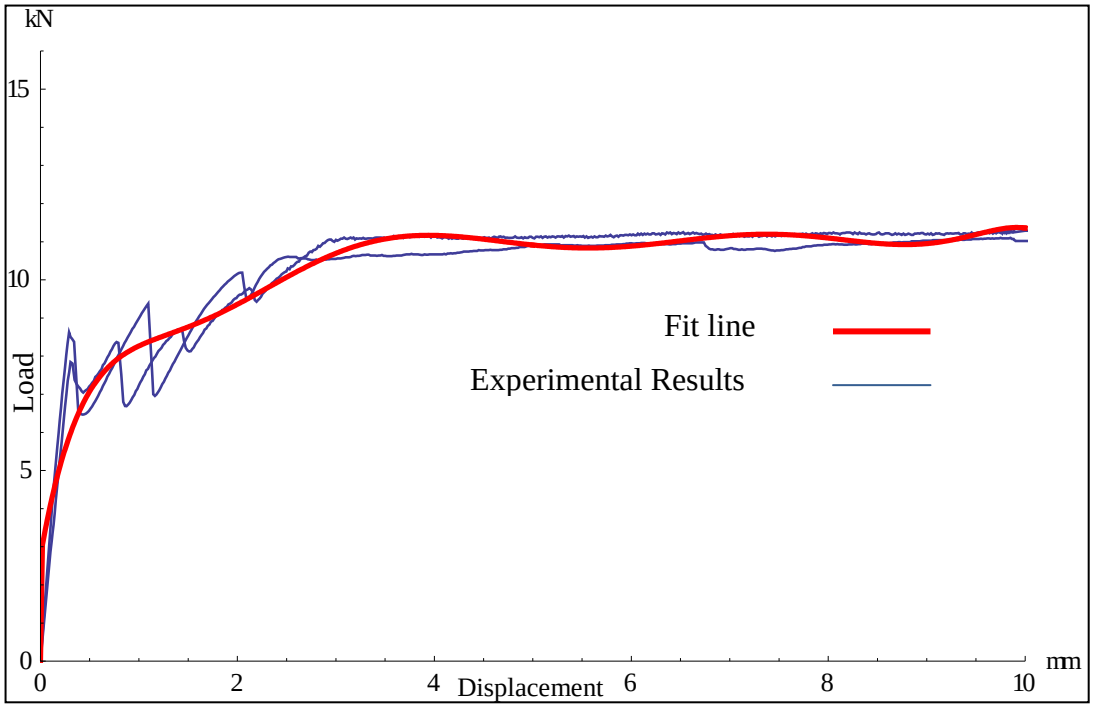

Figure 23. Load- Deflection Diagram:RC Slab 0.5% Fiber (AR60)

The flexural capacity in specimens with 1.0, 1.5, and 2.0% fibers, subsequent to reach the maximum value, initiated to decrease.

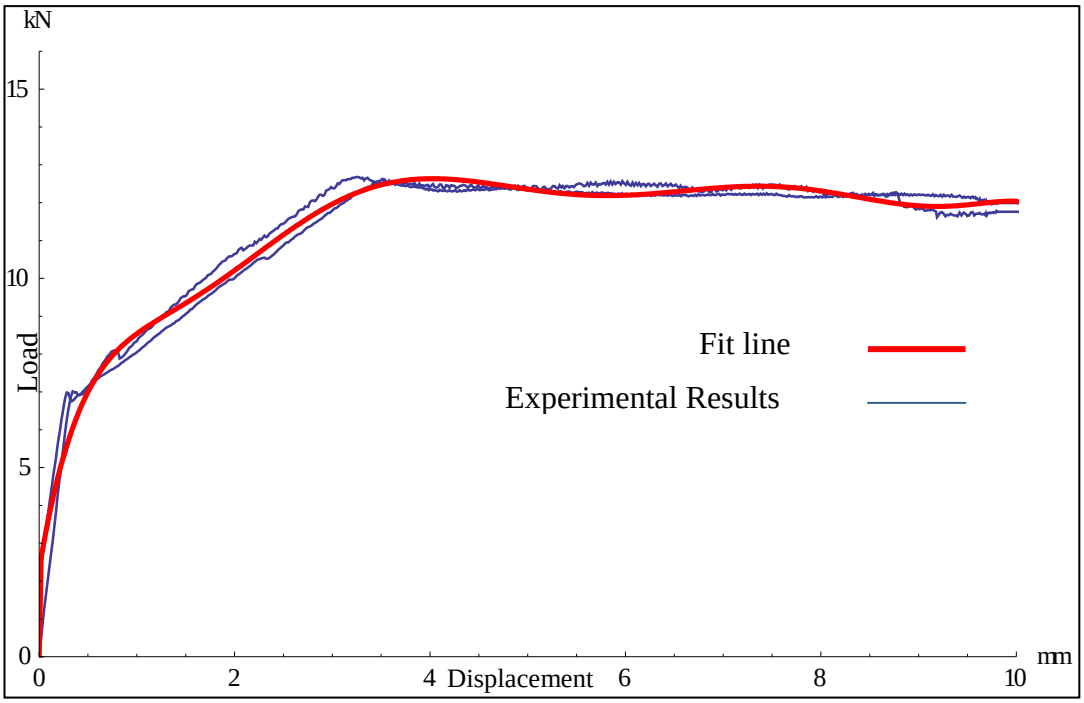

Figure 24. Load- Deflection Diagram:RC Slab 1.0% Fiber (AR60)

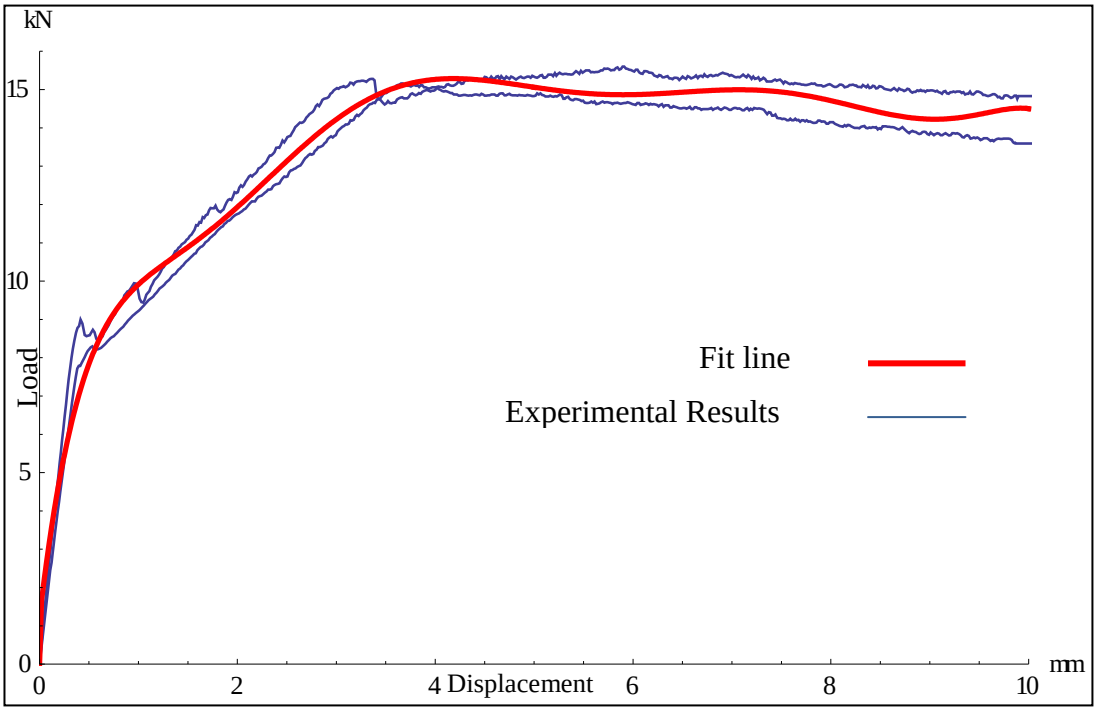

Figure 25. Load- Deflection Diagram:RC Slab 1.5% Fiber (AR60)

The primary effects of fibers on flexural behavior of slab strips with 1.0, 1.5, and 2.0 per cent demonstrated the considerable enhancement in stiffness.

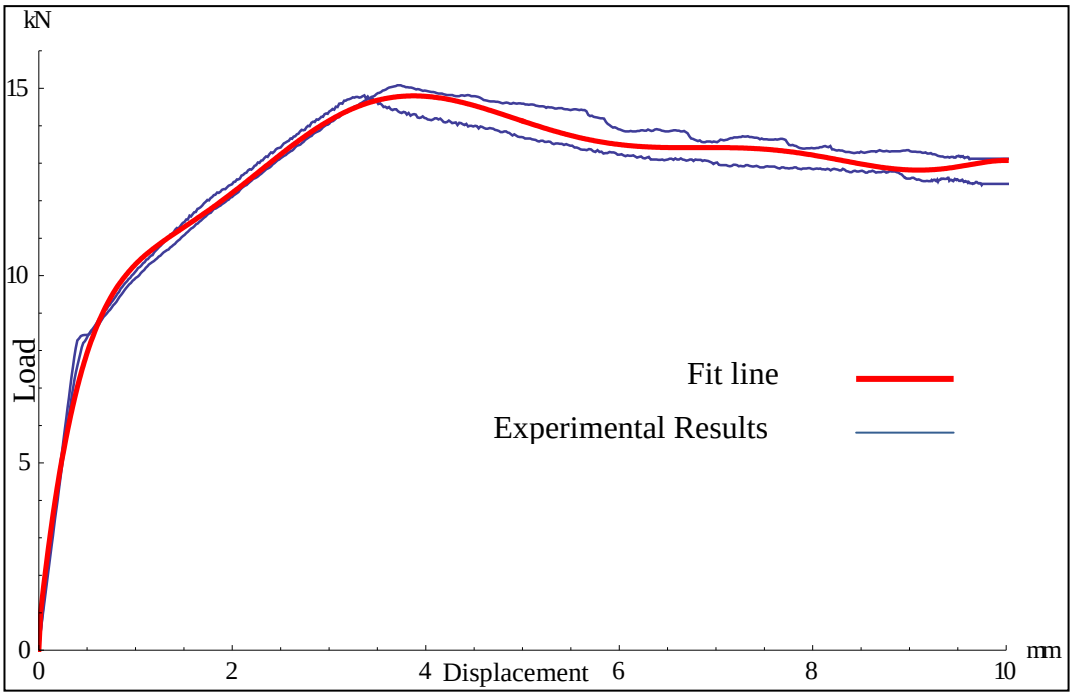

Figure 26. Load- Deflection Diagram:RC Slab 2.0% Fiber (AR60)

In Figure 27, a comparison between mean fit lines of different specimens with aspect ratio 60 fiber is shown. In zone B, the crack propagation region, there have been stiffness enhancements with increasing the fiber percentage. However, the improvement of this region, for specimens with 1.5% and 2.0% fibers are approximately identical.

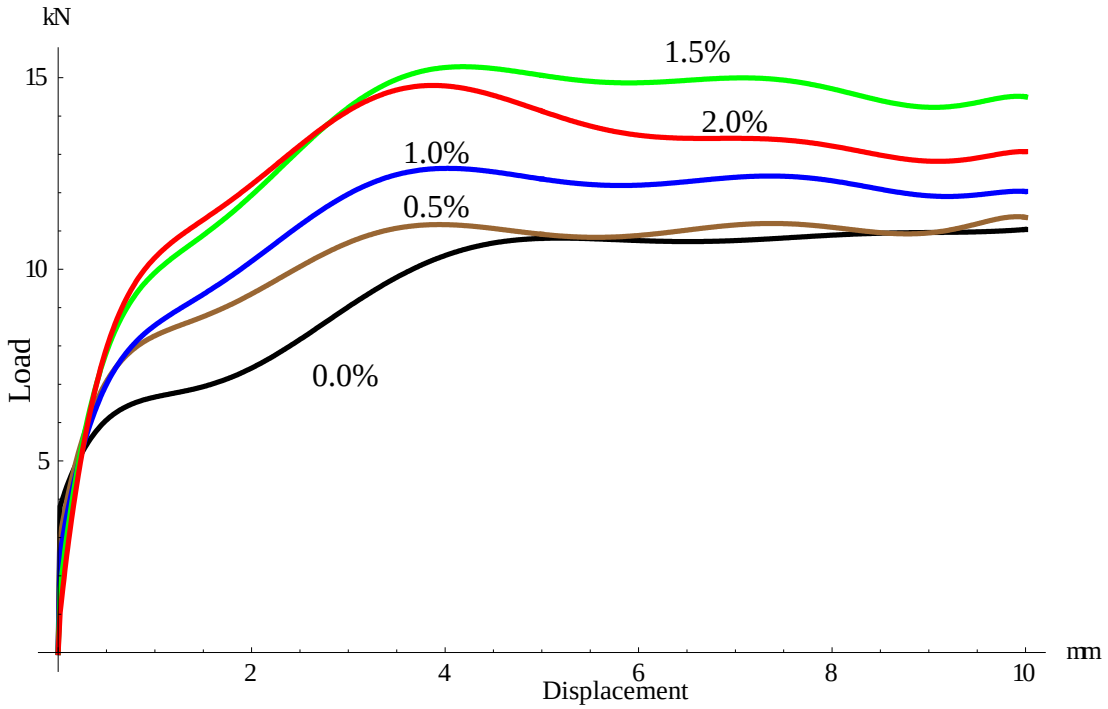

Figure 27. Comparative Load- Deflection Diagrams:With and without fibers (AR80)

Furthermore, for AR60 fibers, the post- cracking strengths of specimens with 2.0% fiber were less than specimens with 1.5% fiber content in concrete. The reason for this phenomenon could be effect of fibers on bonding between bars and concrete (Figure 27).

In addition, the improvement in flexural behavior subsequent to the pick flexural strength for specimen with 0.5% were insignificant, and the most efficient dosage of fibers were 1.5% to enhance the post cracking strength (Figure 28).

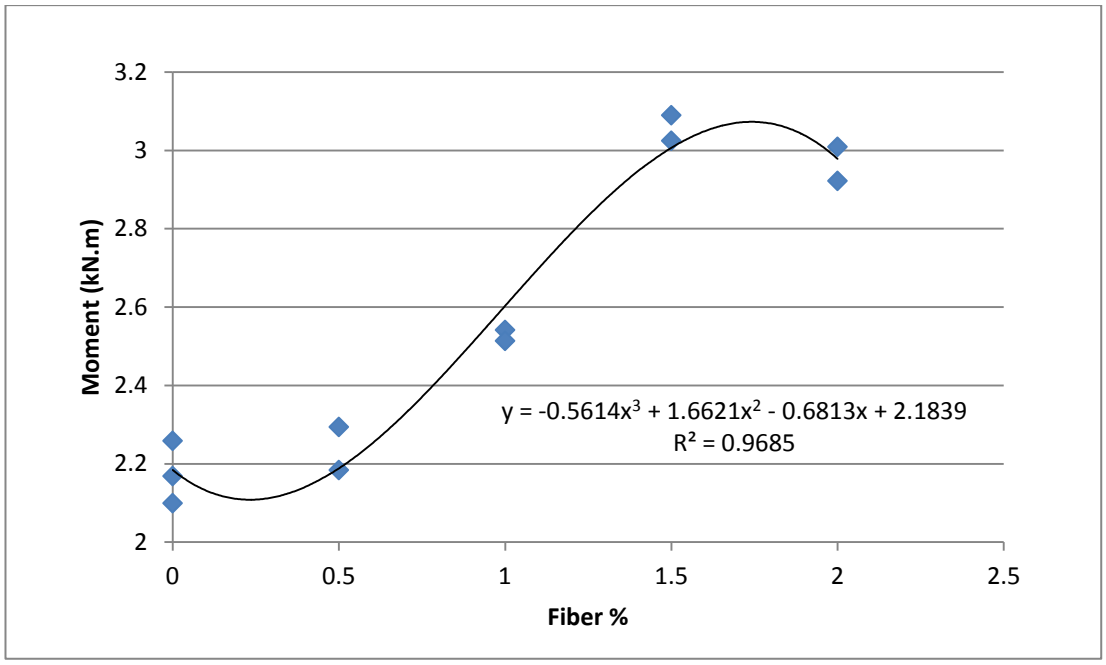

Figure 28. Flexural Enhancement Trend (AR60)

4.1.4 Flexural Energy Absorption

The SFRC reinforced slabs potential for absorbing the energy during the flexural test results represent the ductility index for seismic design. However, seismic behavior of SFRC reinforced slab is beyond this research scope, energy consuming ability of slabs could be essential step to investigate their seismic performance.

To calculate the energy absorption, numerical integration via Mathematica (Wolfram-Research-Inc., 1988-2011) has been applied on flexural results. The average energy absorptions according to type and percentage of fibers are illustrated in Table 3.

Table 3. Average Energy Absorption

Fiber Type	Fiber %	0.0%	0.5%	1.0%	1.5%	2.0%
AR(80)		95.606*	107.461	124.579	145.309	148.412
AR(60)		95.606*	102.700	112.904	134.777	127.214

* The units are kN.mm

According to Table 3, both type of fibers have been affected the flexural stiffness and enhance the energy absorption capacity. Fibers with aspect ratio 80 by 0.5, 1.0, 1.5, and 2.0% dosages have 12.4, 30, 52, and 55 per cent improvement respectively, and compared to slab strips without fiber, fibrous slab with aspect ratio 60 fibers, by equal dosages to AR80 specimens were exhibited 7, 18, 40, and 33 percentage enhancements in energy absorption capacity, respectively. By considering the numerical results in table 3, the fibers with aspect ratio 80 have been more efficient than fibers with aspect ratio 60.

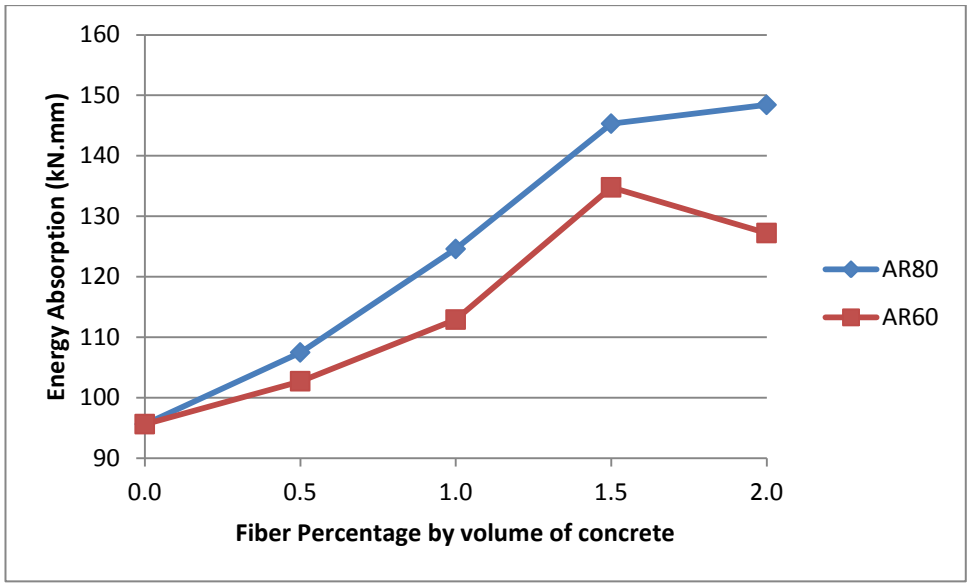

Figure 29. Average Energy Absorption

4.2 Experimental results of flexural test until Concrete Collapse

4.2.1 The flexural test until reaching the maximum deflection

As it was stated in previous chapter, the flexural test machine has been limited to record displacement until 10 mm, and by loading and unloading procedure the fracture of slab strips has been followed. The failure criterions for reinforced concrete members are to yield the reinforcements and to crash concrete in

compression. For detecting the collapse in concrete the visual method was used, and after each cycle of loading the slab strips were inspected. For whole specimens, loading and unloading were pursued to reach the maximum 30mm that the concrete fracture has been observed (Figure 32). After synchronization both data loggers' data, typical diagram that is shown in Figure 30 was produced for each specimen.

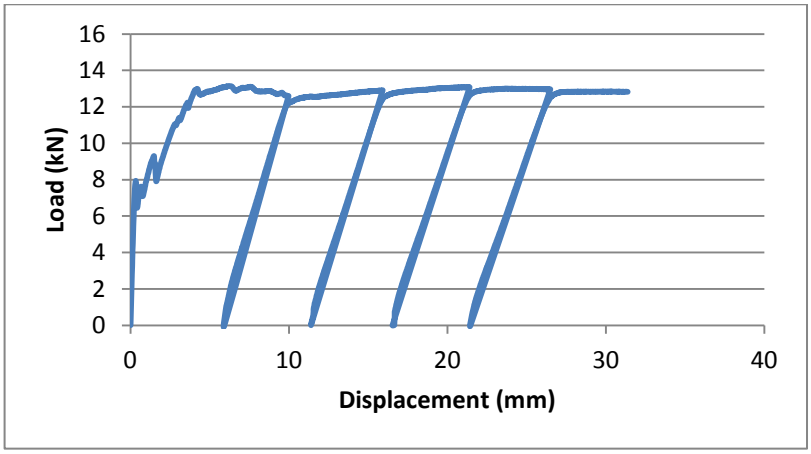

Figure 30. Typical load-unloading-deflection diagram

To weigh up the post-cracking flexural characteristics of SFRC reinforced concrete slabs, the fit line on a trend line has been used and the unloading region has been neglected (Figure 31).

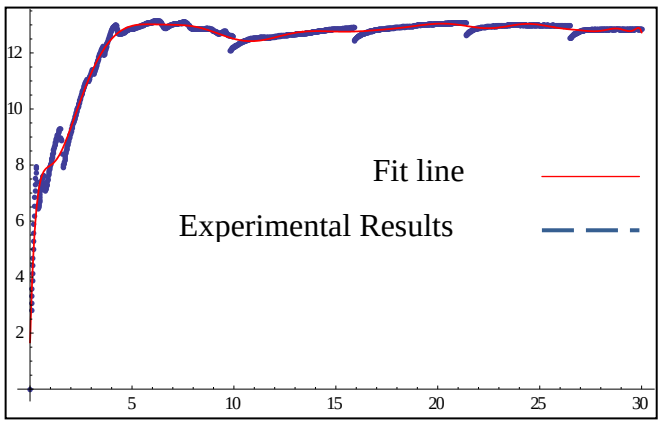

Figure 31. Typical trend fit line

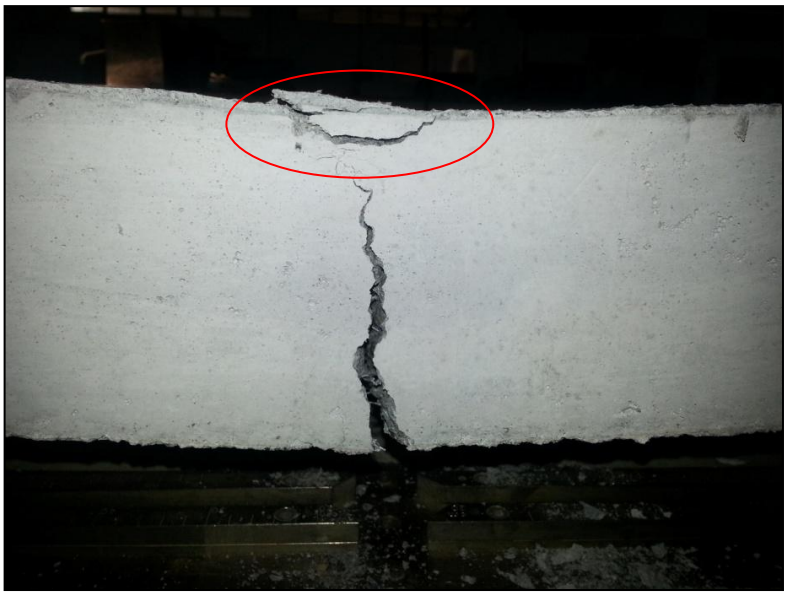

Figure 32. Compressive Collapse of Concrete

By synchronization of parallelized data loggers, 2 load-deflection charts that describe the post-cracking mechanical performance of SFRC reinforced concrete strips have been provided. In Figure 33, the results of flexural test illustrate that the specimens

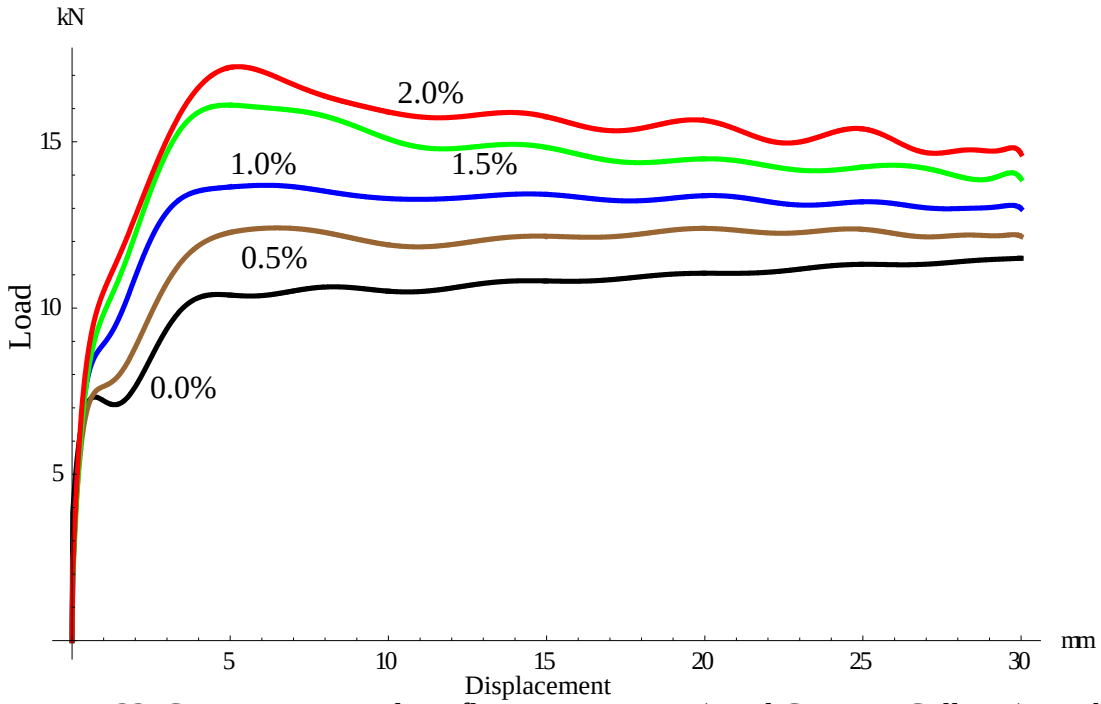

Figure 33. Comparative Load- Deflection Diagrams (Until Concrete Collapse): With and without fibers (AR80)

with 0.5 and 1.0 % fibers (AR80) had steady trend in flexural capacity before observing the compressive fracture. Furthermore, the slab strips without fibers has demonstrated a slight increase in flexural capacity due to hardening of longitudinal reinforcement, and for samples with 1.5 and 2.0 percentages of fibres have maintained the post-cracking strength of specimens.

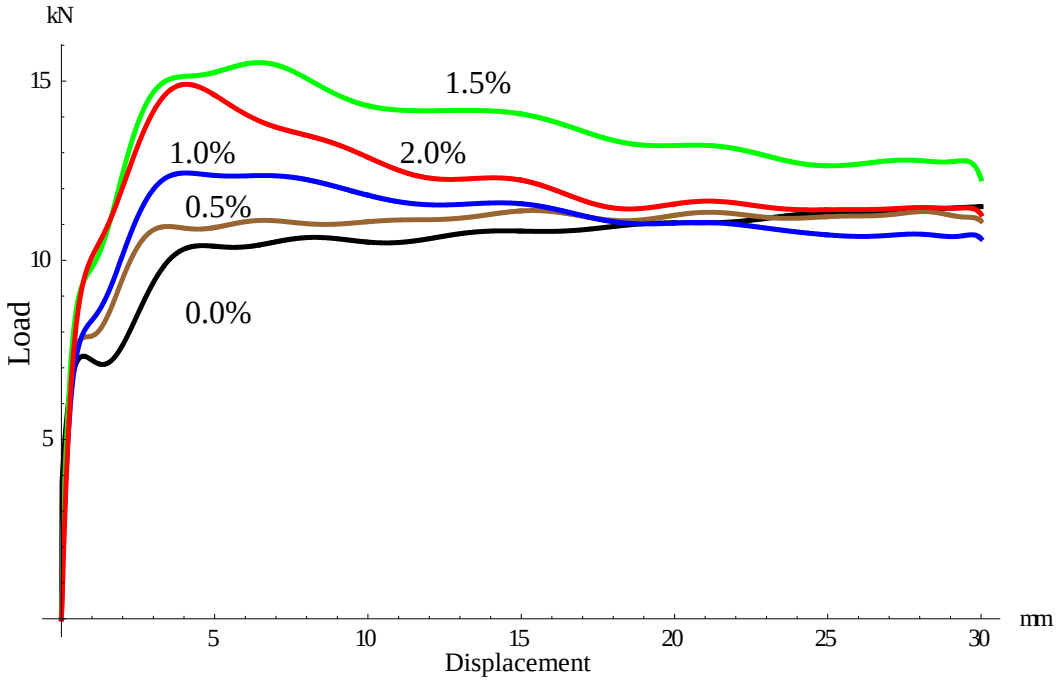

Figure 34. Comparative Load- Deflection Diagrams (Until Concrete Collapse): With and without fibers (AR60)

The AR80 fibers significantly have influenced the mechanical properties and post-cracking rheology of fibrous slabs, in the contrary, the effects of AR60 fibers on after the crack propagation were insignificant. Although, the specimens with 1.5% fibers have shown excellent post-cracking strength in slabs, other dosages of fiber in mixture have been less efficient and seldom improved the pick flexural strength.

4.2.2 Ultimate energy absorption of slabs in flexure

As it was referred in previous section, ultimate conditions to determine the fracture of slabs are yielding the longitudinal reinforcement and crashing the concrete in compression. In this case, the slabs were subjected to controlled-displacement load and by visual inspection, after reaching the 30 mm middle strips deflection the failure in concrete slabs were observed.

The primary method to evaluate the flexural performance of slabs and investigate the effect of fibers on flexural stiffness is energy absorption concept which is simply defined as area under load-displacement curvature. By numerical integration of averaged experimental data, the magnitude of energy that was consumed by each specimen during the deformation has been calculated.

Table 4. Ultimate Energy Absorption

Fiber Type	Fiber %	0.0%	0.5%	1.0%	1.5%	2.0%
AR(80)		315.727*	352.710	388.071	430.741	456.222
AR(60)		315.727*	327.199	334.776	404.892	364.295

* The units are kN.mm

As it is shown in Table 4, compared to fibers with aspect ratio 60, AR80 fibers increase the capacity of energy absorption by 8, 15, 6, and 25% respective to 0.5, 1.0, 1.5, 2.0% dosages of fiber in concrete mixtures, and these results represent the higher performance of fibers with higher aspect ratio.

Moreover, the AR80 fibers have improved the flexural toughness in comparison with specimens without fibers by 12, 23, 36, and 44% and AR60 fibers enhancements have been 3, 6, 28, and 15% regarding the fibers dosages.

4.3 Numerical Simulation of Slab Strips

As it has been demonstrated in previous chapter, to model slab strips via FEA package, compressive and tensile constitutive models which are proposed by Barros (1999) and Sujivorakul (2012), are employed.

4.3.1 Effect of meshing size on numerical result

Although in finite element approach, meshing size could affect the convergence of results. The influence of meshing on load-deformation chart is negligible due to displacement-controlled load. Moreover, 2 different meshing sizes have been examined to investigate meshing size effect.

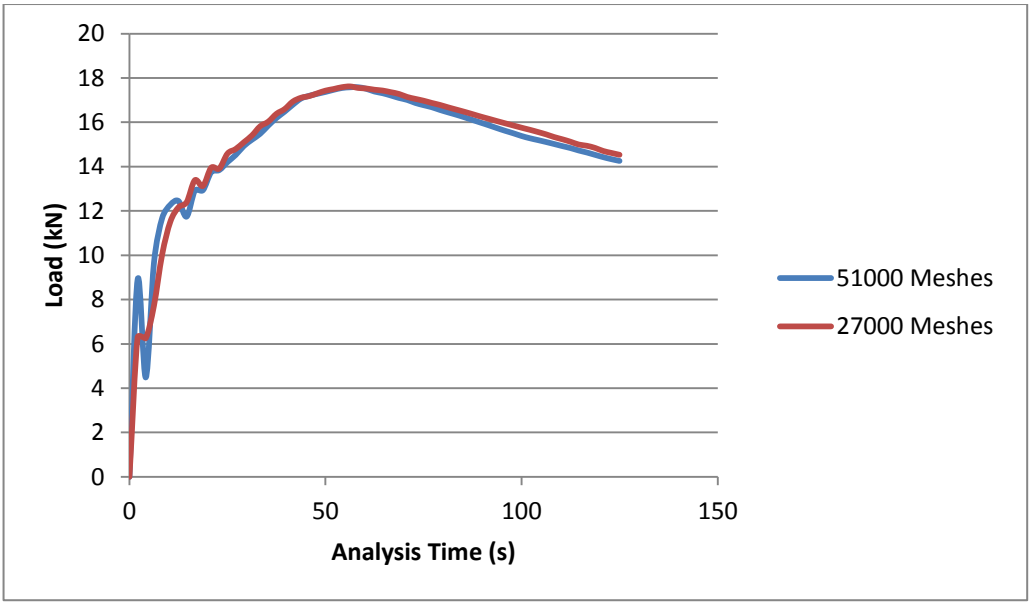

Figure 35. Load-Time diagram during the analysis with divers meshing sizes of slabs

In Figure 35, the diversity of results with changing the meshing size is insignificant, and the initial zone effected slightly.

On the other hand, the maximum stress in concrete elements directly depends on meshing size, and smaller mesh size leads to higher stress due to stress concentration.

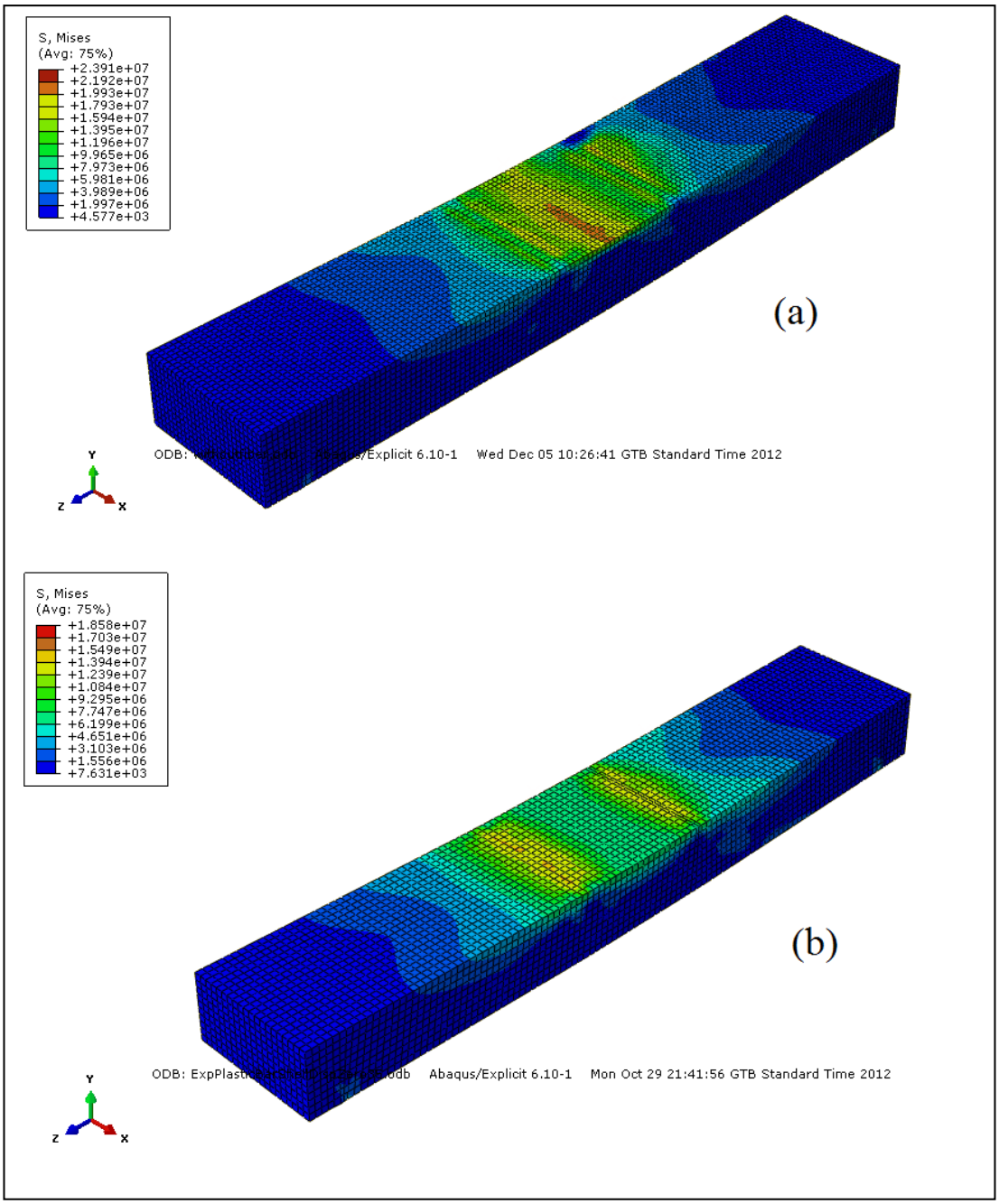

Figure 36. Stress distribution in slab strips: a- 51000 meshes, b- 22600 meshes

Two slab strips without any fiber have been shown in Figure 36, and the meshing sizes were different in them. Although difference in stresses was obvious, compatibility in numerical and experimental load-deflection graphs have been observed. In addition, all the slabs have been analyzed according to maximum 10

mm middle span displacement because the mechanical characteristic of unloaded concrete was not available.

The range of stress in longitudinal reinforcement is shown in Figure 37. In all cases, steel bar has been yielded but the stress level had not reached to fracture stress on steel bar.

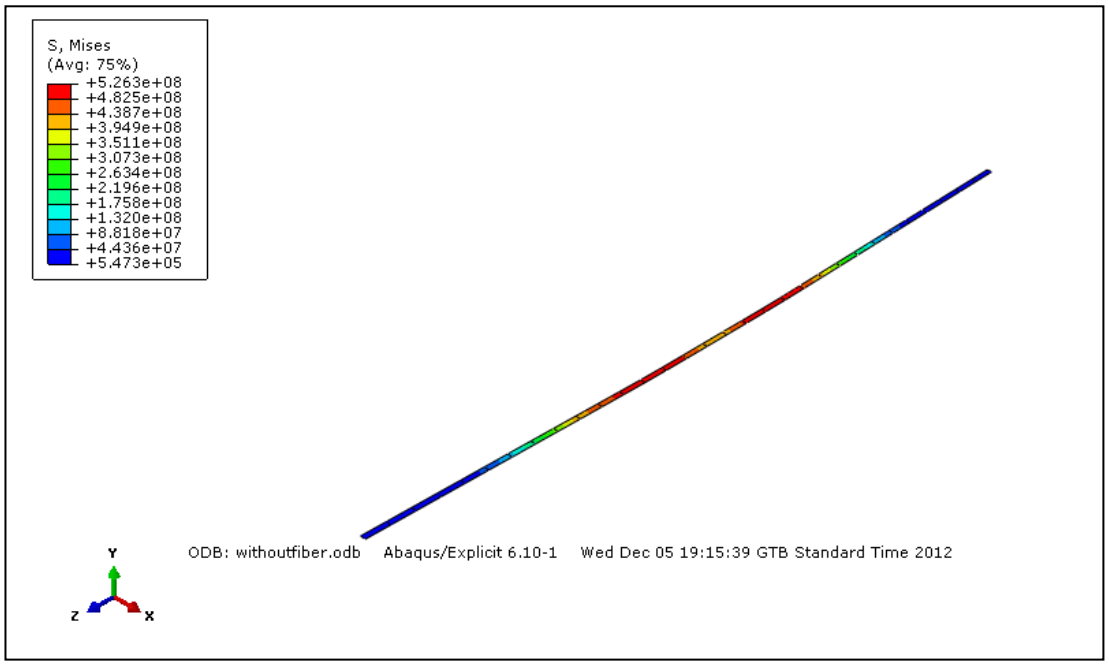

Figure 37. Steel Reinforcement stress distribution

Mesh size in rebar has a local effect on concrete element due to higher stiffness of steel. According to Eriksson and Gasch (2010) recommendation, the mesh size has been chosen somehow to avoid the coincidence of steel and concrete nodes, and it prevents the stress concentration on concrete.

4.3.2 Numerical and experimental load-deflection results

4.3.2.1 Slabs without fibers

To weigh up the experimental results and the theoretical curves, the yielding point, cracking initiation point, and general trends have been considered. In Figure 38, the results for specimen without fibers have been illustrated. The black line introduced the numerical analysis which is in the range of minimum values after yielding point. In addition, tendency of numerical has followed the experimental results, and verified.

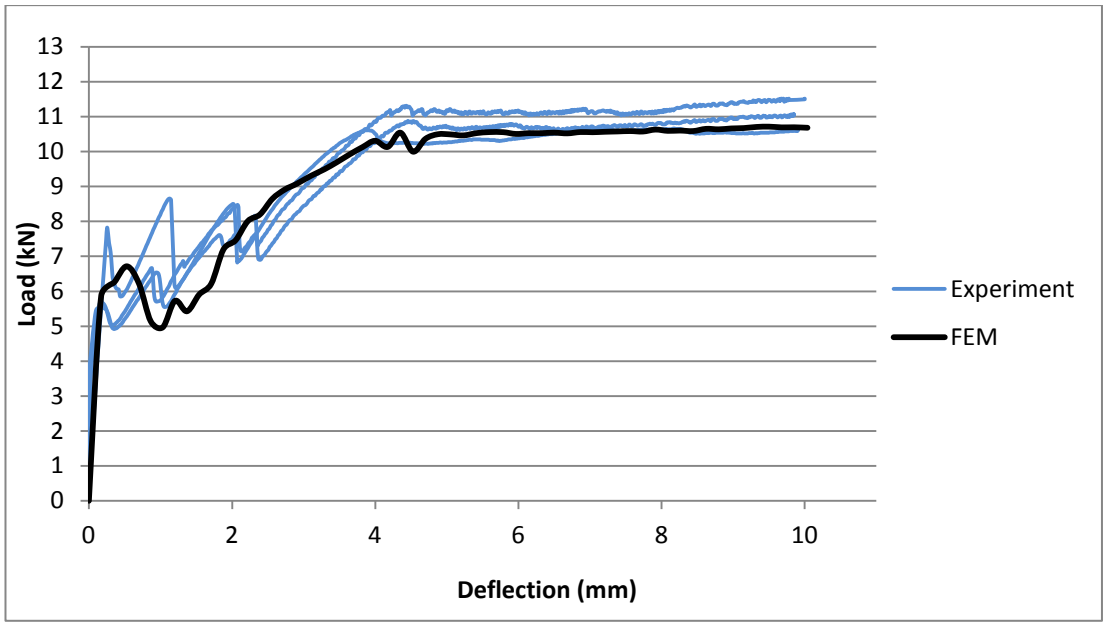

Figure 38. Theoretical and experimental curves- Slab Strips without fiber

4.3.2.2 Fibrous slabs with AR80 fibers

In chapter 3, the primary difference between input data has been explained. Each specimen has diverse material properties due to presence of fibers in concrete mixture. However compressive and tensile models have been changed simultaneously, the effect of tensile models of concrete on flexural stiffness and load-deflection graphs have been more significant.

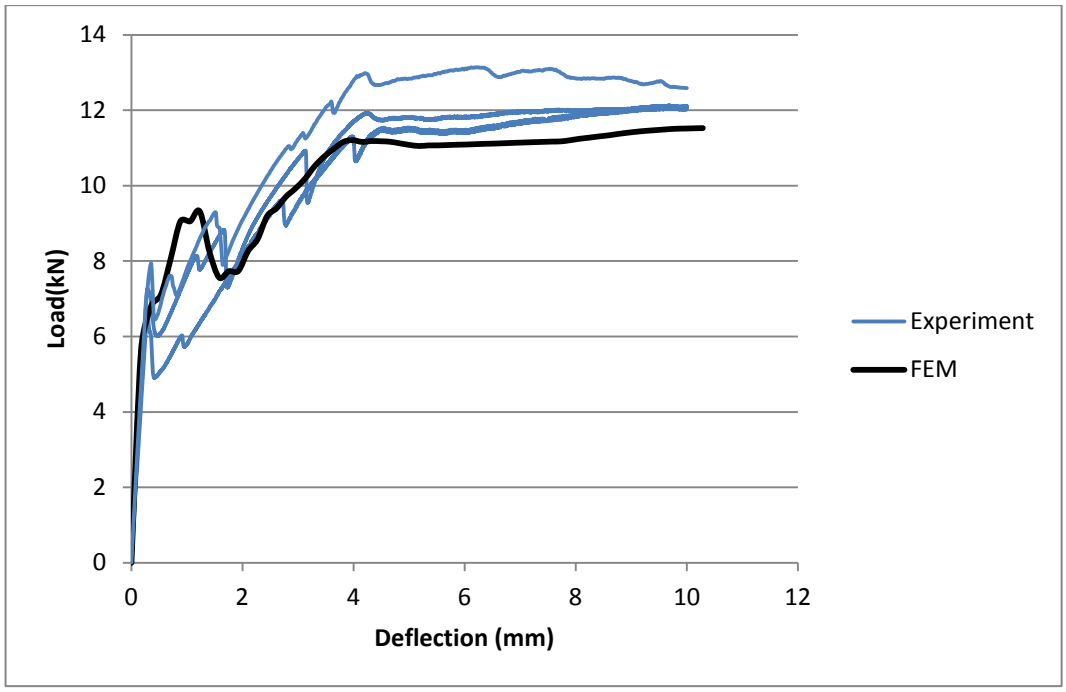

Figure 39. Theoretical and experimental curves- Slab Strips with 0.5% Fiber (AR80)

Tensile model of slabs with diverse percentage AR80 fibers was defined by elastic tensile and post-cracking stress. The numerical load-displacement diagrams have been shown in Figure 39 to 42.

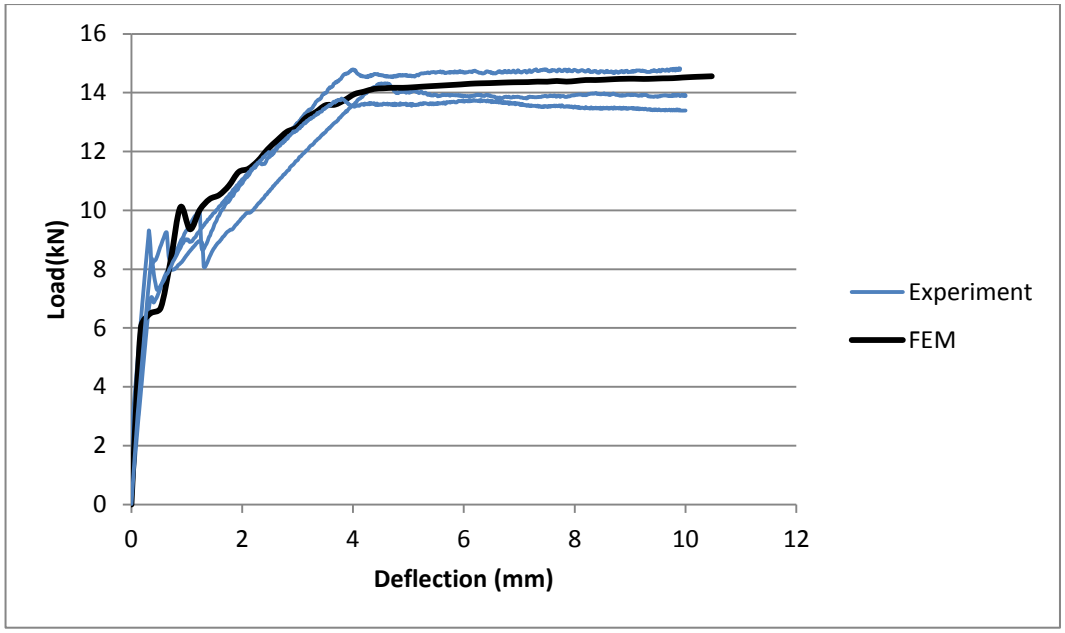

Figure 40. Theoretical and experimental curves- Slab Strips with1.0% Fiber (AR80)

In specimens with 1.0 and 1.5 % AR80 fibers, the tensile behavior of material model has been improved by presence of fibers. The theoretical load-displacements of slab strips have exhibited an acceptable compatibility (Figure 40, Figure 41).

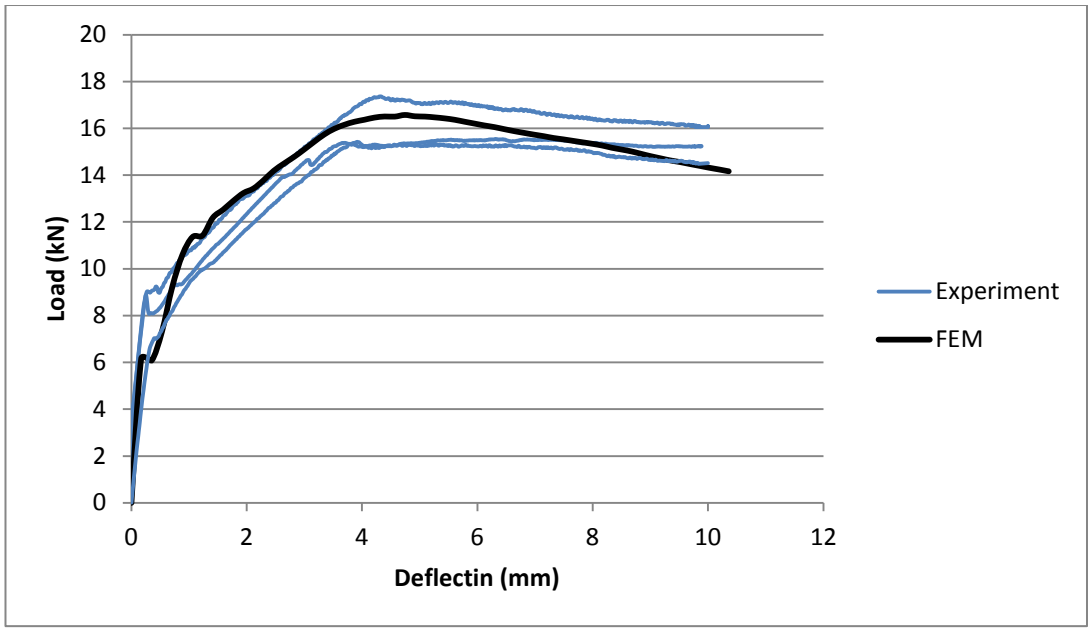

Figure 41. Theoretical and experimental curves- Slab Strips with 1.5% Fiber (AR80)

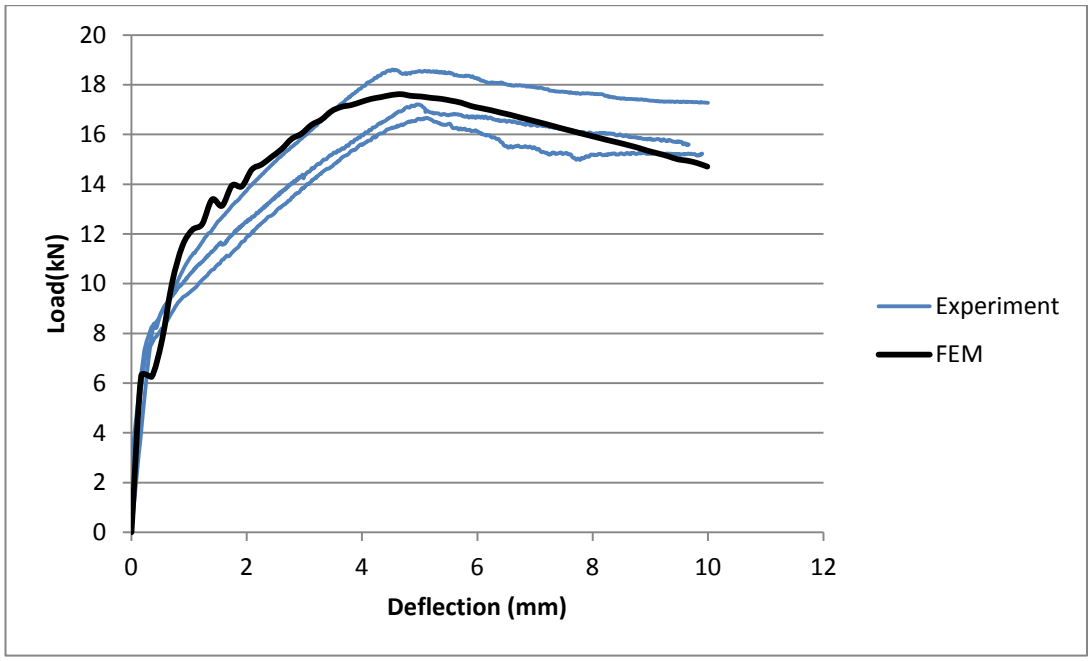

Figure 42. Theoretical and experimental curves- Slab Strips with 2.0% Fiber (AR80)

The tensile models that have been utilized in numerical investigation were defined by Equation 2.19 to 2.24 in chapter two. Although, these models that were proposed by Sujivoraku (2012), Meskenas and Ulbinas (2011), and Naaman (2003) are developed for specimen with maximum 1.5 percentage of fiber in concrete content, for specimens with 2.0% fiber participation, the tensile model was extrapolation and its accuracy for AR80 has been illustrated in Figure 42. According to numerical result of slab strips with 2.0% AR80 fibers, compared to experimental load- deflection curve, there has been higher stiffness during the crack propagation zone and pervious to reach the maximum load capacity.

4.3.2.3 Fibrous slabs with AR60 fibers

Compared to AR80, post-cracking performance of specimens with AR60 fibers has been less efficient. In addition, the tensile models that have been suggested by majority of researchers represent the lower concrete tensile stress for lower aspect ratio.

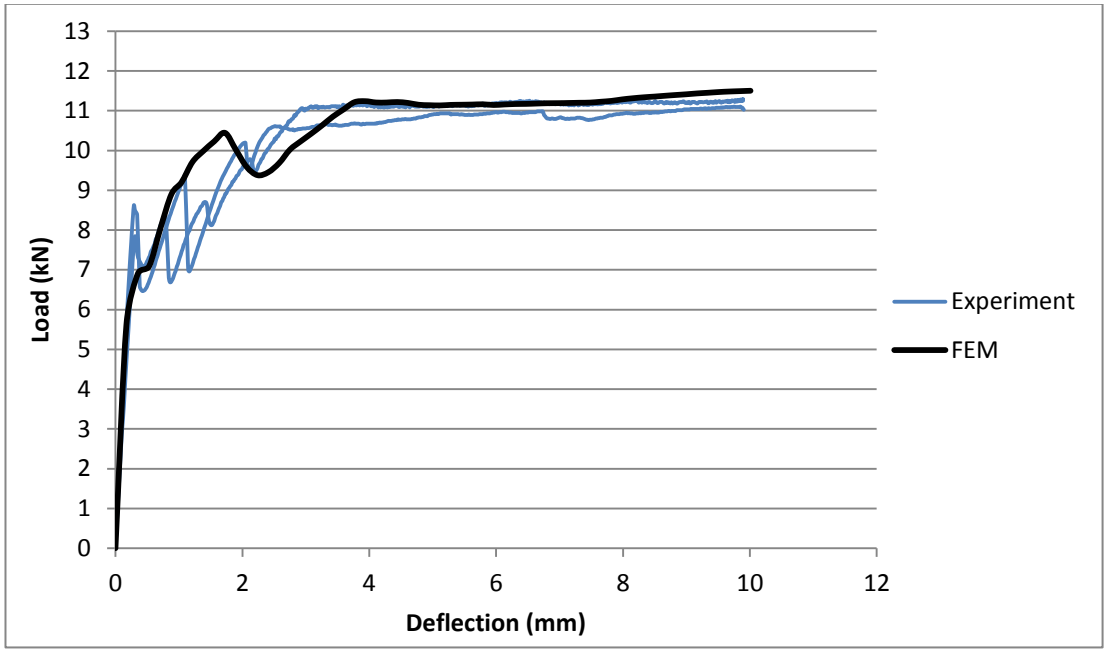

Figure 43. Theoretical and experimental curves - Slab Strips with 0.5% Fiber (AR60)

The experimental results in previous section have demonstrated that the AR80 fibers are more effective than AR60 in flexural strength. Furthermore, the theoretical results of SFRC slabs with AR60 fibers, based on tensile models which were introduced in chapter 2, have been illustrated less compatibility with experimental load-deflection results.

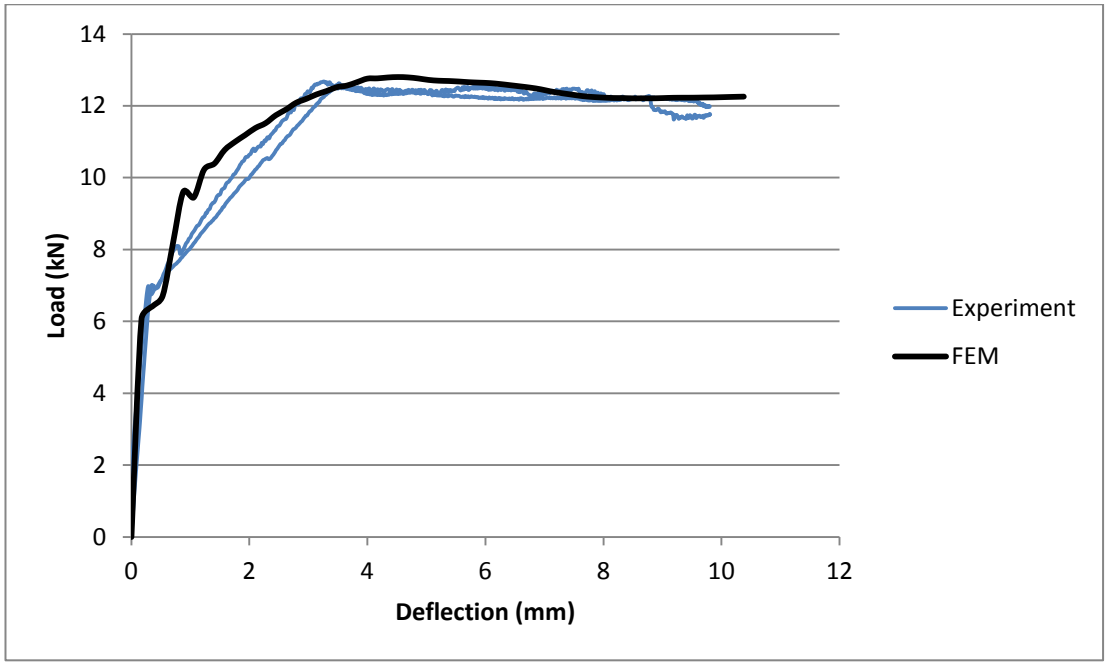

Figure 44. Theoretical and experimental curves - Slab Strips with 1.0% Fiber (AR60)

By 0.5 and 1.0% AR60 fibers dosages, the numerical results have exhibited the higher stiffness than experimental data between elastic displacement and completely yielded region (Figure 43, Figure 44).

The theoretical load-deflection diagrams for fibrous specimens with 1.5 and 2.0% AR60 have been compatible with experimental result until the flexural pick strength, in the contrary, the post- cracking behavior of specimen with 2.0% AR60 fibers has shown higher flexural strength than experimental part (Figure 45, Figure 46).

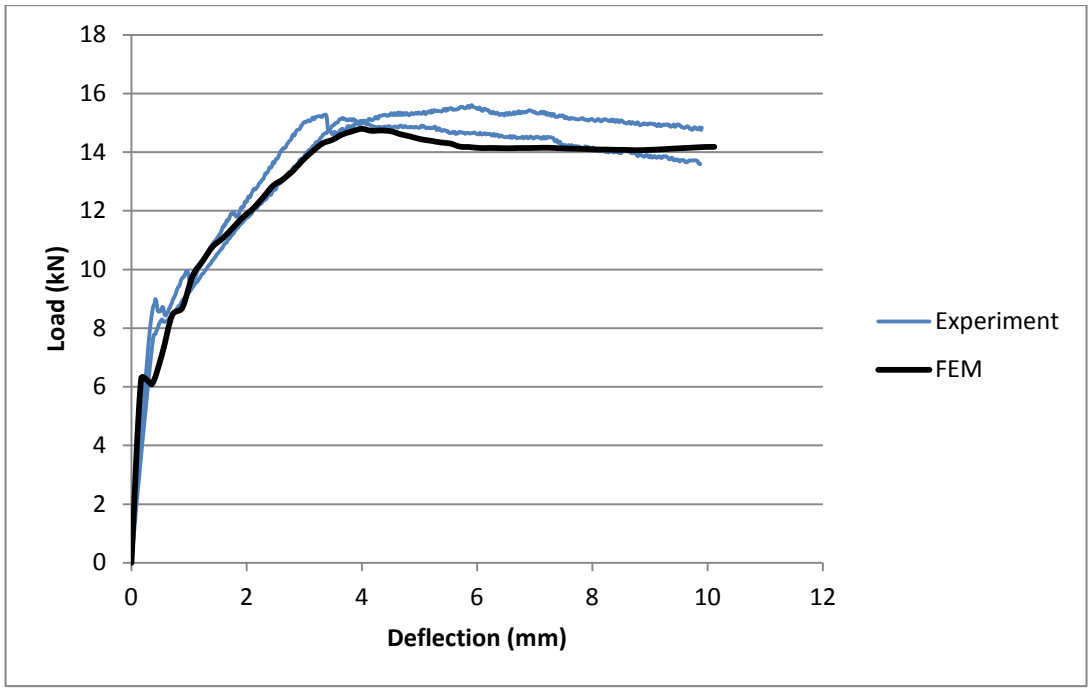

Figure 45. Theoretical and experimental curves - Slab Strips with 1.5% Fiber (AR60)

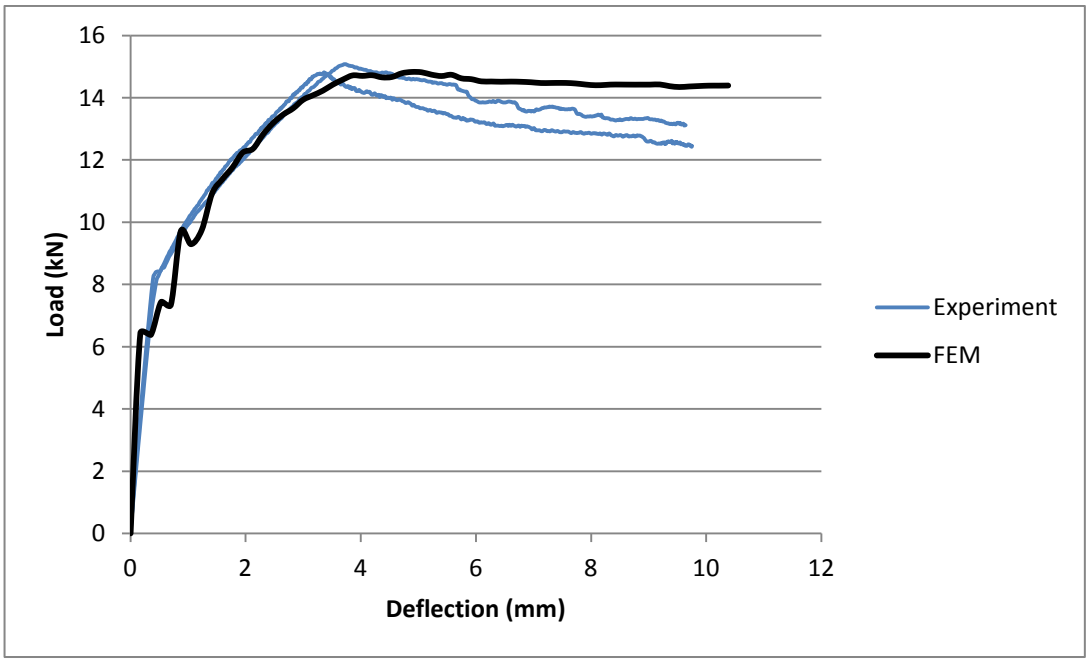

Figure 46. Theoretical and experimental curves - Slab Strips with 2.0% Fiber (AR60)

4.4 Compressive Test Results

The SFRC compressive examinations have illustrated in Figure 1Figure 47and Figure 48, and according to test results by increasing in fiber dosage regardless the fiber type, the post-cracking compressive performance has been enhanced by presence of fibers with maximum 1.5% volumetric fiber content. The slope of stress-strain graphs after ultimate strength pick represents the performance of fibers in compression.

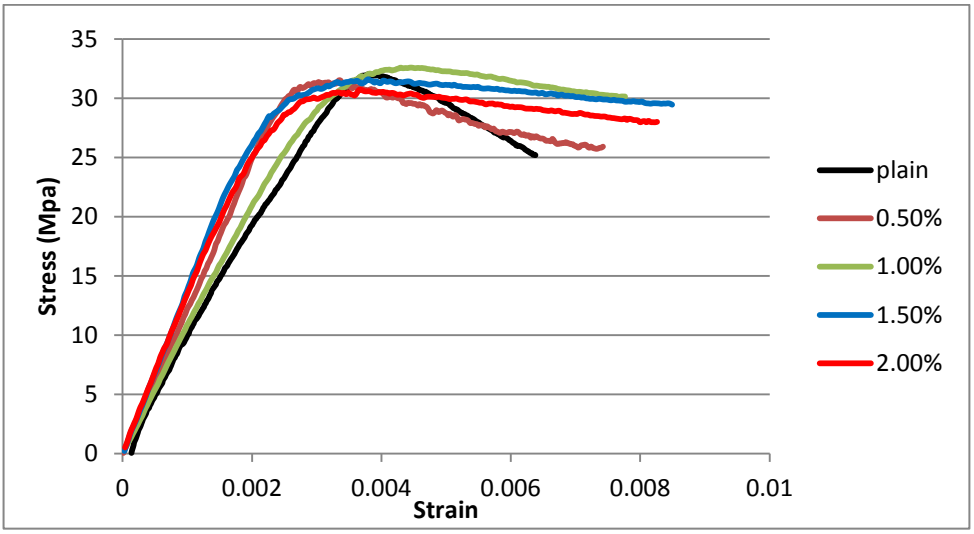

Figure 47. Stress-strain graphs for specimens with AR80 Fiber

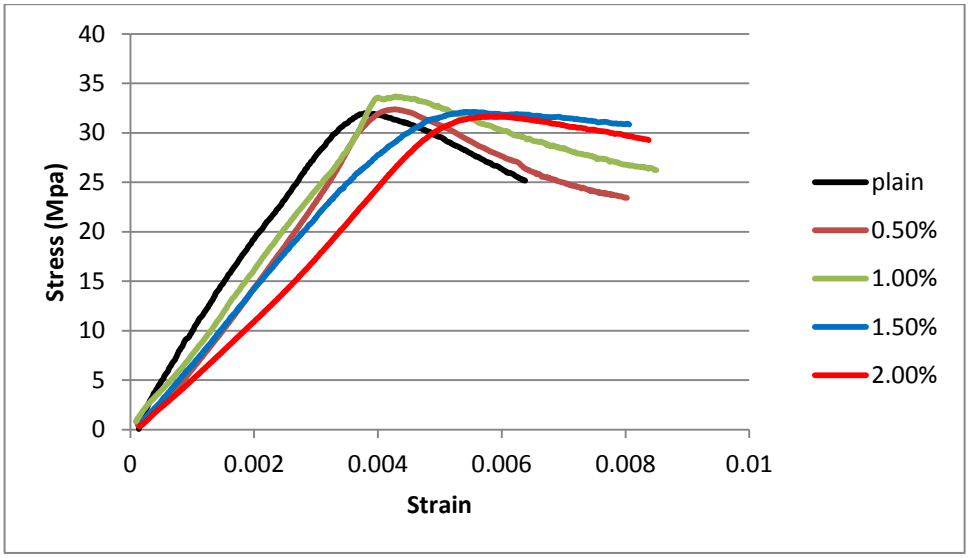

Figure 48. Stress-strain graphs for specimens with AR60 Fiber

4.5 Results discussion summary

The primary influence of fiber on reinforced concrete slabs has been escalation in energy consumption of SFRC slab strips during the loading. Fibers with aspect ratio 80 have enhanced the post-cracking behavior of slabs significantly, and the energy absorption in post-cracking region significantly has been improved.

Theoretical simulation of SFRC slabs based on tensile models that are proposed by Sujivoraku (2012) and Naaman (2003) have been satisfactory accurate to predict the post-cracking rheology of SFRC.

Although these tensile models have based on direct tensile experiment and developed for specimens without longitudinal reinforcement, the suggested equations could be utilized for reinforced slabs and the theoretical results have been compatible with experimental investigation.

Chapter 5

CONCLUSION AND PERSPECTIVES

Since this research has been based on experimental and numerical investigations, the numerical module outcomes should be verified by experimental results, and experiment results have been highly compatible with FEM analysis outcomes. In addition, the experimental results have indicated that the enhancement of mechanical performance due to presence of fibers has been significant.

5.1 Conclusions

Several conclusions are listed in following. In this section it has been tried to summarize the important points of results discussion briefly.

1. The ultimate flexural strength entirely has been affected by utilization of fibers. The experimental results have shown that the fibers with higher aspect ratio were more efficient, and Figure 22, in previous chapter, has been illustrated the flexural performance of slab strips with aspect ratio 80 fibers. Furthermore, increasing in flexural capacity of slabs with aspect ratio 60 fibers has reached to pick point at 1.5 % fibers (Figure 28).
2. To evaluate the post-cracking behavior of fibrous slab strips with traditional reinforcement, energy absorptions of each specimen during the loading have been calculated, and according the results which have been demonstrated in Chapter 4, pick of flexural enhancement in fibrous specimens has been

observed by using 1.5 and 2.0 % fibers in concrete content for fibers with aspect ratio 60 and 80, respectively.

3. Energy absorptions of fibrous slabs have increased from up to 55% of specimen without steel fibers in concrete (by utilization of aspect ratio 80 fibers).
4. The primary result that has been concluded from numerical modeling of fibrous slab strips is that current constitutive models for tensile and compression of fibrous reinforced concrete which have been proposed by previous researchers (Barros & Figueiras, 1999) and (Sujivorakul, 2012) have enough accuracy to employ in theoretical modeling of structural members. However, post-cracking behavior of models with 2.0 % fibers have exhibited a higher flexural capacity. These results have indicated that the ultimate and post-cracking mechanical characteristics of fibrous concrete that have been predicted by direct tensile test overestimates the results.
5. The loading and unloading test results have illustrated that subsequent to reach the maximum flexural strength, the load capacity of specimens decreased. However, the drops in load-displacement curvatures have been smaller for fibrous specimens with aspect ratio 80 fibers.
6. Despite the fact that the mechanical improvement of concrete due to effects of fibers on tensile and compressive stress of concrete are neglected by majority of building codes, according to numerical and experimental results and their compatibility with each others, it could be considered that the mechanical improvement of concrete material in flexural design are significant.

5.2 Future Studies

This research could be a background for deriving the stress-strain relationship of steel fibrous concrete compatible with FEM analysis tools. In addition, the seismic performance of SFRC frames could be investigated to evaluate the compatibility of theoretical model with structural application of SFRC members.

REFERENCES

ACI318. (2011). *Building Codes Requirements for Structural Concrete (ACI318-11) and commentary.* American Concrete Institute.

ACI544. (1999). *Design Considerations for Steel Fiber Reinforced Concrete.* American Concrete Institute.

ACI544. (2002). *Report on Fiber Reinforced Concrete.* American Concrete Institute.

Altun, F., Haktanir, T., & Ari, K. (2007). Effects of steel fiber addition on mechanical properties of concrete and RC beams. *Construction and Building Materials, 21*, 654–661.

Ashour, S. A., Wafa, F. F., & Kamal, M. I. (2000). Effect of the concrete compressive strength and tensile reinforcement ratio on the flexural behavior of fibrous concrete beams. *Engineering Structures, 22*, 1145–1158.

ASTM-C39. (2004). *Standard Test Method forCompressive Strength of Cylindrical Concrete Specimens.* ASTM International.

Barros, J., & Figueiras, J. (1999). Flexural behavior of steel fiber reinforced concrete:testing and modelling. *Journal of Materials in Civil Engineering, ASCE, 11*, 331-339.

Basu, P. C., Shylamoni, P., & Roshan, A. D. (2004). Characterisation of steel reinforcement for RC structures: An overview and related issues. *The Indian Concrete Journal*, 19-30.

Bencardino, F., Rizzuti, L., Spadea, G., & Swamy, N. R. (2008). Stress-Strain Behavior of Steel Fiber-Reinforced Concrete in Compression. *JOURNAL OF MATERIALS IN CIVIL ENGINEERING*, 255-263.

Brandt, A. M. (2008). Fibre reinforced cement-based (FRC) composites after over 40 years of development in building and civil engineering. *Composite Structures, 86*, 3-9.

Chiaia, B., Fantilli, A. P., & Vallini, P. (2009). Combining fiber-reinforced concrete with traditional reinforcement in tunnel linings. *Engineering Structures, 31*, 1600-1606.

Dhakal, R., & Song, H. (2005). *EFFECT OF BOND ON THE BEHAVIOR OF STEEL FIBRE REINFORCED CONCRETE BEAMS.* Christchurch: Department of Civil Engineering, University of Canterbury,.

Eriksson, D., & Gasch, T. (2010). *FEM-modeling of reinforced concrete and verification of the concrete material models available in ABAQUS.* Stockholm: Royal Institute of Technology.

Gribniak, V., Kaklauskas, G., Hung Kwan, A. K., Bacinskas, D., & Ulbinas, D. (2012). Deriving stress–strain relationships for steel fibre concrete in tension from tests of beams with ordinary reinforcement. *Engineering Structures,* 387–395.

Hibbit, H., Karlsson, B., & Sorensen, E. (2009). *Abaqus 6.9 Online Documentation.*

Junior, L., Borges, V., Danin, A., Machado, D., Araujo, D., Debs, M., & Rodrigues, P. (2010). Stress-strain curves for steel fiber-reiforced concrete in compression. *Materia, 15*.

Khaloo, A. R., & Afshari, M. (2005). Flexural behaviour of small steel fibre reinforced concrete slabs. *Cement & Concrete Composites 27*, 141-149.

Mangat, P., & Motamedi Azarit, M. (1984). Influence of steel fibre reinforcement on fracture behaviour of concrete in compression. *The International Journal of Cement Composites and Lightwight Concrete, 6*, 219-232.

Marar, K., Eren, Ö., & Yitmena, İ. (2011). Compression Specific Toughness of Normal Strength Steel Fiber Reinforced Concrete (NSSFRC) and High Strength Steel Fiber Reinforced Concrete (HSSFRC). *Materials Research*, 239-247.

Marsh, B. K. (1988). *Design of normal concrete mixes.* Watford: Building Research Establishment.

Meskenas, A., & Ulbinas, D. (2011). Discrete crack model of steel fibre reinforced concrete members subjected to tension. *14th Lithuanian Conference of Young*

Scientists "Science - Future of Lithuania". Lithuanian : Vilnius Gediminas Technical University.

Özcan, D. M., Bayraktar, A., Sahin, A., Haktanir, T., & Türker, T. (2009). Experimental and finite element analysis on the steel fiber-reinforced concrete (SFRC) beams ultimate behavior. *Construction and Building Materials, 23*, 1064–1077.

Rieder. (n.d.). *Archi Tonic*. Retrieved from http://www.architonic.com/

Šalna, R., & Marčiukaitis, G. (2010). INFLUENCE OF FIBER SHAPE ON THE STRENGTH OF STEEL FIBER REINFORCED CONCRETE. *Modern Building Materials, Structures, and Techniques*, 764-767.

Shetty, M. (2005). *The concrete technology, theory and practice.* New Delhi: S. Chand and Company LTD.

Simulia Abaqus/CAE 6.11. (2011). Dassault Systèmes Simulia Corp.

Soranakom, C., & Mobasher, B. (2009). Flexural Design of Fiber-Reinforced Concrete. *ACI MATERIALS JOURNAL*, 461-469.

Sujivorakul, C. (2012). Model of Hooked Steel Fibers Reinforced Concrete under Tension. In G. P. Montesinos, H. Reinhardt, & A. Naaman, *High Perfomance Fiber Reinforced Cement Composits 6* (pp. 19-26).

Telford, T. (1993). *CEB-FIP Model Code 1990.* Euro-International Concrete Committee.

Twintec. (n.d.). *Twintec Industrial Flooring*. Retrieved from http://www.twintec.co.uk

Wolfram-Research-Inc. (1988-2011). Wolfram Mathematica 8.0. *Wolfram Research Inc.*

Zollo, R. F. (1997). Fiber-reinforced Concrete: an Overview after 30 Years of Development. *Cement and Concrete Composites, 19*, 107-122.